

1 **The hidden role of dissolved organic carbon in the**
2 **biogeochemical cycle of carbon in modern redox-stratified**
3 **lakes**

4 Robin Havas^{a,*}, Christophe Thomazo^{a,b}, Miguel Iniesto^c, Didier Jézéquel^d, David Moreira^e, Rosaluz Tavera^e,
5 Jeanne Caumartin^f, Elodie Muller^f, Purificación López-García^e, Karim Benzerara^f
6

7 ^a Biogéosciences, CNRS, Université de Bourgogne Franche-Comté, 21 000 Dijon, France

8 ^b Institut Universitaire de France, 75005 Paris, France

9 ^c Ecologie Systématique Evolution, CNRS, Université Paris-Saclay, AgroParisTech, 91190 Gif-sur-Yvette,
10 France

11 ^d IPGP, CNRS, Université Paris Cité, 75005 Paris, and UMR CARTELE, INRAE & USMB, France

12 ^e Departamento de Ecología y Recursos Naturales, Universidad Nacional Autónoma de México, México

13 ^f Sorbonne Université, Muséum National d'Histoire Naturelle, CNRS, Institut de Minéralogie, de Physique des
14 Matériaux et de Cosmochimie (IMPMC), 75005 Paris, France.
15

16

17

18 * *Correspondence to:* Robin Havas (robin.havas@gmail.com)

19

20

21

22

23 *Keywords: Carbon cycle; isotopic fractionation; DOC; Precambrian analogues*

24 **Abstract.** The dissolved organic carbon (DOC) reservoir plays a critical role in the C cycle of marine and
25 freshwater environments because of its size and implication in many biogeochemical reactions. Although it is
26 poorly constrained, its importance in ancient Earth's C cycles is also commonly invoked. Yet DOC is rarely
27 quantified and characterized in modern stratified analogues. In this study, we investigated the DOC reservoirs of
28 four redox-stratified alkaline crater lakes in Mexico. We analyzed the concentrations and isotopic compositions of
29 DOC throughout the four water columns and compared them with existing data on dissolved inorganic and
30 particulate organic C reservoirs (DIC and POC). The four lakes have high DOC concentrations with great
31 variability between and within the lakes (averaging 2 ± 4 mM; 1SD, n=28; i.e. from ~ 15 to 160 times the amount
32 of POC). The $\delta^{13}\text{C}_{\text{DOC}}$ signatures also span a broad range of values from -29.3 to -8.7 ‰ (with as much as 12.5 ‰
33 variation within a single lake). The prominent DOC peaks (up to 21 mM), together with their associated isotopic
34 variability, are interpreted as reflecting oxygenic and/or anoxygenic primary productivity through the release of
35 excess fixed carbon in three of the lakes (La Alberca de los Espinos, La Preciosa, and Atexcac). By contrast, the
36 variability of [DOC] and $\delta^{13}\text{C}_{\text{DOC}}$ in the case of Lake Alchichica is mainly explained by the partial degradation of
37 organic matter and accumulation of DOC in anoxic waters. The DOC records detailed metabolic functions such as
38 active DIC-uptake and DIC-concentrating mechanisms, which cannot be inferred from DIC and POC analyses
39 alone, but which are critical to the understanding of carbon fluxes from the environment to the biomass.
40 Extrapolating our results to the geological record, we suggest that anaerobic oxidation of DOC may have caused
41 the very negative C isotope excursions in the Neoproterozoic. It is however unlikely that a large oceanic DOC
42 reservoir could outweigh the entire oceanic DIC reservoir. This study demonstrates how the analysis of DOC in
43 modern systems deepens our understanding of the C cycle in stratified environments and helps to set boundary
44 conditions for the Earth's past oceans.

45

46

47 1. INTRODUCTION

48 Dissolved organic carbon (DOC) is a major constituent of today's marine and freshwater environments (e.g.
49 Ridgwell and Arndt, 2015; Brailsford, 2019). It is an operationally defined fraction of aqueous organic carbon
50 within a continuum of organic molecules spanning a broad range of sizes, compositions, degrees of reactivity, and
51 bioavailability (Kaplan et al., 2008; Hansell, 2013; Beaupré, 2015; Carlson and Hansell, 2015; Brailsford, 2019).
52 Oceanic DOC is equivalent to the total amount of atmospheric carbon (Jiao et al., 2010; Thornton, 2014) and
53 represents the majority of freshwater organic matter (Kaplan et al., 2008; Brailsford, 2019). The DOC reservoir is
54 (i) at the base of many trophic chains (Bade et al., 2007; Hessen and Anderson, 2008; Jiao et al., 2010; Thornton,
55 2014), (ii) key in physiological and ecological equilibria (Hessen and Anderson, 2008) and (iii), has a critical role
56 for climate change as a long-term C storage reservoir (Jiao et al., 2010; Hansell, 2013; Thornton, 2014; Ridgwell
57 and Arndt, 2015). Although isotopic signatures are a powerful and widespread tool in biogeochemical studies, the
58 use of DOC isotopes has been relatively limited owing to technical difficulties (Cawley et al., 2012; Barber et al.,
59 2017). Radioisotopes or labeled stable isotopes of DOC have been used to date and retrace DOC compounds in
60 diverse aquatic environments (e.g. Repeta and Aluwihare, 2006; Bade et al., 2007; Kaplan et al., 2008; Brailsford,
61 2019). Studies featuring natural abundances of DOC stable isotope data (i.e. $\delta^{13}\text{C}_{\text{DOC}}$) mainly used them to
62 discriminate between different source endmembers (e.g. terrestrial vs. autochthonous) (e.g. Cawley et al., 2012;
63 Santinelli et al., 2015; Barber et al., 2017). After a pioneer study by Williams and Gordon (1970), few studies have
64 used natural DOC stable isotope compositions to explore processes intrinsically related to its production and
65 recycling. Recently, Wagner et al. (2020) reaffirmed the utility of stable isotopes to investigate DOC biosynthesis,
66 degradation pathways, and transfer within the foodweb.

67 Several studies have suggested a significant role for the DOC reservoir throughout geological time, when it would
68 have been much larger in size and impacting various phenomena, including: the regulation of climate and
69 glaciations during the Neoproterozoic (e.g. Peltier et al., 2007), the paleoecology of Ediacaran Biota and its early
70 complex life forms (e.g. Sperling et al., 2011), the oxygenation of the ocean through innovations of eukaryotic life
71 near the Neoproterozoic-Cambrian transition (e.g. Lenton and Daines, 2018), and the perturbation of the C cycle
72 recorded in $\delta^{13}\text{C}$ sedimentary archives from the Neoproterozoic to the Phanerozoic (e.g. Rothman et al., 2003; Fike
73 et al., 2006; Sexton et al., 2011; Ridgwell and Arndt, 2015).

74 The contribution of DOC reservoirs to the past and modern Earth's global climate and biogeochemical cycles
75 remains poorly constrained (Jiao et al., 2010; Sperling et al., 2011; Dittmar, 2015; Fakhraee et al., 2021) and the
76 existence and consequences of a large ancient oceanic DOC are still debated (e.g. Jiang et al., 2010, 2012; Ridgwell
77 and Arndt, 2015; Li et al., 2017; Fakhraee et al., 2021). Thus, in addition to modeling approaches (e.g. Shi et al.,
78 2017; Fakhraee et al., 2021), the understanding of DOC-related processes in the past anoxic and redox-stratified
79 oceans (Lyons et al., 2014; Havig et al., 2015; Satkoski et al., 2015) should rely on the characterization of DOC
80 dynamics in comparable modern analogues (Sperling et al., 2011). Although many studies have explored the C
81 cycle of modern redox-stratified environments (e.g. Crowe et al., 2011; Kuntz et al., 2015; Posth et al., 2017;
82 Schiff et al., 2017; Havig et al., 2018; Cadeau et al., 2020; Saini et al., 2021; Petrash et al., 2022), very few have
83 analyzed DOC and even fewer have measured its stable isotope signature (Havig et al., 2018).

84 In this study, we characterize the DOC reservoir of four modern redox-stratified alkaline crater lakes from the
85 Trans-Mexican Volcanic Belt (Ferrari et al., 2012) and its role within the C cycle of these environments. We report

86 DOC concentration and isotopic composition at multiple depths in the four water columns, and discuss these results
87 in the context of physico-chemical parameters (temperature, dissolved oxygen, chlorophyll a, and nutrient
88 concentrations), and the isotopic composition of dissolved inorganic and particulate organic carbon (DIC, POC),
89 all measured in the same lakes and from the same water samples as in Havas et al. (2023). The four lakes show
90 distinct water chemistries, along an alkalinity/salinity gradient (Zeyen et al., 2021), with diverse planktonic
91 microbial communities (Iniesto et al., 2022; Havas et al., 2023). These characteristics allow us to examine the
92 effect of specific environmental and ecological constraints on the production and recycling of DOC in redox
93 stratified environments. We then present how the analysis of DOC deepens our understanding of the C cycle in
94 these lakes, compared to more classical DIC and POC analyses. Finally, the production and fate of the DOC
95 reservoir in these modern analogues is used to discuss the potential role of DOC in past perturbations of the
96 sedimentary C isotope record from the Neoproterozoic and Phanerozoic.

97

98 2. SITE DESCRIPTION

99 The main characteristics of the geological, climatic and limnological context of the lakes under study are presented
100 here, but a more detailed description is available in Havas et al. (2023).

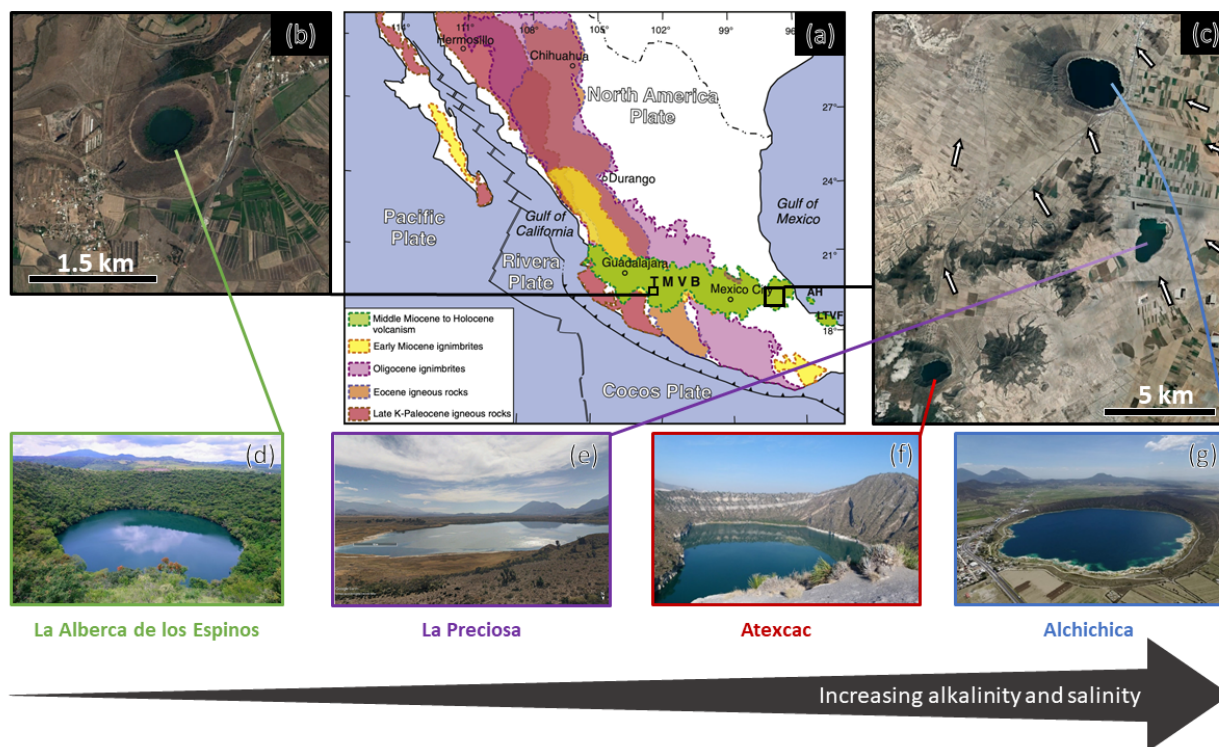
101 The four lakes are volcanic maars formed after phreatic, magmatic and phreatomagmatic explosions, and are
102 located in the Trans-Mexican Volcanic Belt (TMVB, Fig. 1). The first lake, La Alberca de los Espinos, is located
103 at the margin of the Zacapu tectonic lacustrine basin in the Michoacán-Guanajuato Volcanic Field (MGVF), in the
104 western-central part of the TMVB (Fig. 1). The other three (La Preciosa, Atexcac, and Alchichica) are located
105 within the same zone (~ 50 km²) of the Serdan-Oriental Basin (SOB), in the easternmost part of the TMVB (Fig. 1).
106 La Alberca, with a temperate semi-humid climate, is predominantly underlain by andesitic rocks (Siebe et al.,
107 2012, 2014). By contrast, Alchichica shows much higher evaporation than precipitation rates, reflecting the
108 temperate sub-humid to temperate arid climate experienced by the SOB lakes (Silva-Aguilera et al., 2022). These
109 lakes overlie calcareous and basaltic/andesitic basement rocks (Carrasco-Núñez et al., 2007; Chako Tchamabé et
110 al., 2020).

111 These variations in geological context and hydrological processes generate a gradient of water chemical
112 compositions, where salinity, alkalinity and DIC increase in the following order: (i) Lake La Alberca, (ii) La
113 Preciosa, (iii) Atexcac, and (iv) Alchichica (Zeyen et al., 2021). The four lakes are alkaline with pH values around
114 9. Under these conditions, DIC is composed of HCO₃⁻/CO₃²⁻ ions with minor amounts of CO_{2(aq)} (< 0.5 %). This
115 favors the precipitation of microbialite deposits, which are found in the four systems but more abundantly as
116 alkalinity increases (Zeyen et al., 2021).

117 The four lakes are defined as warm monomictic with anoxic conditions prevailing in the bottom waters during
118 most of the year (i.e. one mixing period per year, during winter; Armienta et al., 2008; Macek et al., 2020; Havas
119 et al., 2023). They are all “closed lakes” with no inflow or outflow of surficial waters and are thus fed by rain and
120 groundwater only.

121 Atexcac is the most oligotrophic of the three SOB lakes (Lugo et al., 1993; Vilaclara et al., 1993; Sigala et al.,
122 2017). Chlorophyll a data from May 2019 (Fig. 2), based on mean and maximum value categories (OECD, 1982),
123 indicate ultra-oligotrophic conditions for Atexcac (≤ 1 and 2 µg/L, respectively), oligotrophic for Alchichica (≤ 2

124 and 6 $\mu\text{g/L}$, respectively), intermediate between oligo- and mesotrophic for La Alberca (≤ 3 and 4.5 $\mu\text{g/L}$,
 125 respectively) and “low” mesotrophic for La Preciosa (≤ 3 and 9 $\mu\text{g/L}$, respectively). Total dissolved P
 126 concentrations from May 2019 show similar values for the three SOB lakes close to the surface (increasing in the
 127 anoxic zone of Alchichica) but much higher values for La Alberca (Havas et al., 2023). This pattern was observed
 128 during previous sampling campaigns (Zeyen et al., 2021). La Alberca is surrounded by more vegetation, which
 129 could favor the input of nutrients to this lake. La Preciosa and La Alberca are thus the least oligotrophic of the four
 130 lakes. Importantly, although differences in trophic status exist between the four lakes, they are more oligotrophic
 131 than eutrophic.



132
 133 Figure 1. Geographical location and photographs of the four crater lakes. (a) Geological map from Ferrari et al.
 134 (2012) with black squares showing the location of the four studied lakes within the Trans-Mexican Volcanic Belt
 135 (TMVB). (b, c) Close up © Google Earth views of La Alberca de los Espinos and the Serdan-Oriental Basin
 136 (SOB). The white arrows represent the approximate groundwater flow path (based on Silva-Aguilera, 2019). (d-
 137 g) Photographs of the four lakes (d from © Google Image [‘enamoredemexicowebiste’], e from © Google Earth
 138 street view, and g from © ‘Agencia Es Imagen’). Figure from Havas et al. (2023).

139

140 3. METHOD

141 3.1. Sample Collection

142 All samples were collected in May 2019. Samples for DOC analyses were collected at different depths from the
 143 surface to the bottom of the water columns, particularly where the physico-chemical parameters showed
 144 pronounced variation (e.g. at the chemocline and turbidity peaks; Fig. 2 and Table 1). Water samples were collected
 145 with a Niskin bottle. For comparison with DIC and POC data, the DOC was analyzed on the same Niskin sampling
 146 as in Havas et al. (2023), except where indicated (Fig. 4; Tables 1 and 2). Analyses of DOC and major, minor, and

147 trace ions were carried out after water filtration at 0.22 μm , directly in the field with Filtropur S filters pre-rinsed
148 with lake water. Details about the sampling procedure and analysis of the physico-chemical parameters, as well as
149 DIC and POC measurements, are reported in Havas et al. (2023).

150

151 **3.2. Dissolved organic carbon (DOC) concentration and isotope measurements**

152 Filtered solutions were acidified to a pH of $\sim 1\text{-}2$ to degas all the DIC and leave DOC as the only C species in
153 solution. The bulk DOC was analyzed directly from the acidified waters (i.e. all organic C molecules smaller than
154 0.22 μm). Bulk concentration was measured with a Vario TOC at the Laboratoire Biogéosciences (Dijon),
155 calibrated with a range of potassium hydrogen phthalate (Acros®) solutions. Before isotopic analysis, DOC
156 concentration of the samples was adjusted to match international standards at 5 ppm (USGS 40 glutamic acid and
157 USGS 62 caffeine). Isotopic compositions were measured at the Laboratoire Biogéosciences using an IsoTOC
158 (Elementar, Hanau, Germany), running under He-continuous flow and coupled with an IsoPrime stable isotope
159 ratio mass spectrometer (IRMS; Isoprime, Manchester, UK). Samples were stirred with a magnetic bar and flushed
160 with He before injection of 1 mL sample aliquots (repeated 3 times). The DOC was then converted into gaseous
161 CO_2 by combustion at 850 $^\circ\text{C}$, quantitatively oxidized by copper oxide and separated from other combustion
162 products in a reduction column and a water condenser. This CO_2 was transferred to the IRMS via an open split
163 device. To avoid a significant memory effect between consecutive analyses, each sample (injected and measured
164 three times) was separated by six injections of deionized water and the first sample measurement was discarded.
165 Average $\delta^{13}\text{C}_{\text{DOC}}$ reproducibility was 1.0 ‰ for standards and 0.5 ‰ for samples (1SD). The average
166 reproducibility for sample [DOC] measurements was 0.3 mM, and blank tests were below the detection limit.

167 In addition to DOC measurements, we calculated the “Total carbon concentration” as the sum of DOC, DIC, and
168 POC concentrations, with DIC and POC data from Havas et al. (2023). The corresponding isotopic composition
169 ($\delta^{13}\text{C}_{\text{Total}}$) was calculated as the weighted average of the three $\delta^{13}\text{C}$. The DIC and POC isotope data were also used
170 to calculate isotopic differences with $\delta^{13}\text{C}_{\text{DOC}}$, expressed in the $\Delta^{13}\text{C}$ notation. The values for $\delta^{13}\text{C}_{\text{DIC}}$ and $\delta^{13}\text{C}_{\text{POC}}$
171 are detailed in Havas et al. (2023) and summarized in the results section.

172

173 **4. RESULTS**

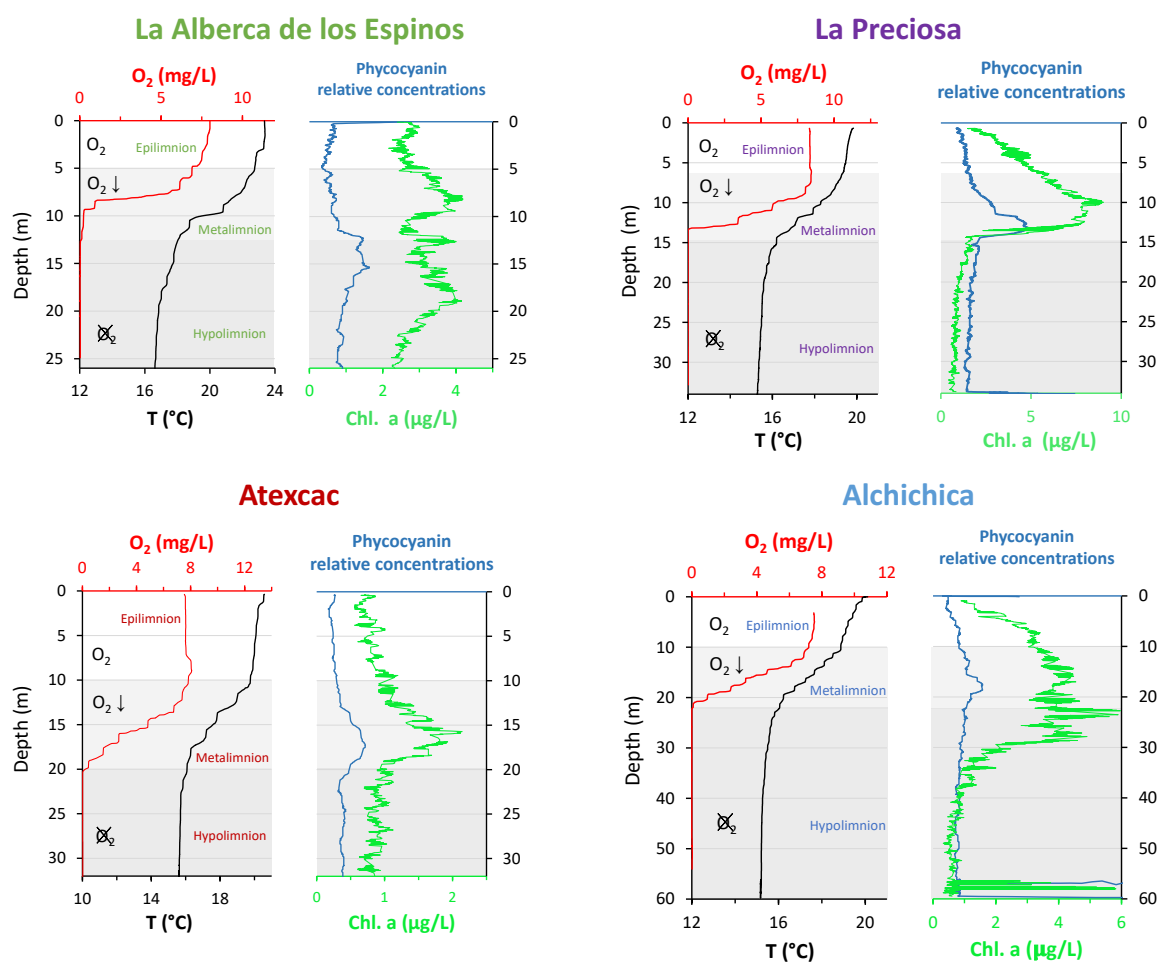
174 The water columns of the four lakes were clearly stratified in May 2019 (Fig. 2; Havas et al., 2023). The epi-,
175 meta-, and hypo-limnion layers of each lake were identified based on the thermocline depths, and correspond to
176 the oxygen-rich, intermediate, and oxygen-poor layers in the four lakes, although the oxycline in La Preciosa is
177 slightly thinner than the thermocline (~ 5 vs. 8 m). In the following, DIC, POC, O_2 , chlorophyll a (Chl a), NH_4 , P
178 and $\text{CO}_{2(\text{aq})}$ data are also presented.

179

180 **4.1. Lake La Alberca de los Espinos**

181 Bulk DOC had a concentration of ~ 0.4 mM throughout the water column, except at 7 and 17 m, where it peaked
182 at 1.0 and 1.7 mM, respectively (Fig. 3). Its isotopic composition ($\delta^{13}\text{C}_{\text{DOC}}$) was comprised between -27.2 and -

183 25.1 ‰ except at 7 m, where it reached -14.7 ‰ (Fig. 3). It represented ~8% of total carbon on average, and 93%
 184 of the organic carbon present in the water column. Total C concentration increased downward from about 7 to
 185 9 mM. The $\delta^{13}\text{C}_{\text{total}}$ decreased from -3.9 to -7.9 ‰ between 5 and 17 m and then increased to -3.2 ‰ at 25 m
 186 (Table 1). The isotopic difference between DOC and DIC ($\Delta^{13}\text{C}_{\text{DOC-DIC}}$) was between -21.2 and -25.2 ‰, except
 187 at 7 m depth, where it peaked to -12.4 ‰ (Fig. 4; Table 2). The $\Delta^{13}\text{C}_{\text{DOC-POC}}$ values were comprised between -1.5
 188 and +3.1 ‰, except at 7 m depth, where DOC was enriched in ^{13}C by ~11.5 ‰ (Fig. 4; Table 2). The DIC
 189 concentration and $\delta^{13}\text{C}_{\text{DIC}}$ averaged 7.5 ± 0.7 mM and -2.9 ± 0.8 ‰; POC concentration and $\delta^{13}\text{C}_{\text{POC}}$ averaged
 190 0.04 ± 0.02 mM and -27.1 ± 1.3 ‰. Dissolved oxygen showed a stratified profile with an oxycline layer
 191 transitioning from O₂-saturated to O₂-depleted conditions between 5 and 12 m depths (Fig. 2). Chl a concentration
 192 showed three distinct peaks at ~7.5, 12.5 and 17.5 m depths, all reaching ~4 $\mu\text{g/L}$ (Fig. 2). The average NH₄⁺ and
 193 P concentrations were 3.9 and 11.3 μM , respectively. The activity of CO_{2(aq)} was 10^{-5.00} at 7 m depth and increased
 194 to 10^{-3.40} at the bottom of the lake.



195 Figure 2. Physico-chemical parameter depth profiles of La Alberca de los Espinos, La Preciosa, Atexcac, and
 196 Alchichica: dissolved oxygen concentration (mg/L), water temperature (°C), phycocyanin and chlorophyll a
 197 pigments ($\mu\text{g/L}$). Absolute values for phycocyanin concentrations were not determined; only relative variations
 198 are represented (with increasing concentrations to the right). Epi-, meta- and hypo-limnion layers are represented
 199 for each lake by the white, gray, and dark gray areas, based on temperature profiles with the metalimnion
 200 corresponding to the thermocline. The three layers match the oxygen-rich, intermediate, and oxygen-poor zones,
 201 except in La Preciosa). Original data from Havas et al. (2023).

202

203 4.2. Lake La Preciosa

204 Bulk DOC had a concentration of ~ 0.5 mM throughout the water column except at 12.5 m, where it peaked at
205 1.6 mM. The $\delta^{13}\text{C}_{\text{DOC}}$ was -25.9 ± 0.4 ‰ throughout the water column except between 12.5 and 15 m, where it
206 reached -20.0 ‰ (Fig. 3). The DOC represented $\sim 3\%$ of the total carbon on average, and 91% of the organic
207 carbon present in the water column. The total C concentration was relatively stable at ~ 13.8 mM, while $\delta^{13}\text{C}_{\text{total}}$
208 was centered around -1 ‰ with a decrease to -2.8 ‰ at 12.5 m (Table 1). The $\Delta^{13}\text{C}_{\text{DOC-DIC}}$ values were very stable
209 with depth around -26 ‰, but markedly increased at 12.5 m up to -19.8 ‰. (Fig. 4; Table 2). The $\Delta^{13}\text{C}_{\text{DOC-POC}}$
210 values decreased from ~ 1.3 ‰ in the upper waters to ~ -0.4 ‰ in the bottom waters but showed a peak to $+7.1$ ‰
211 at a depth of 12.5 m (Fig. 4; Table 2). The DIC concentration and $\delta^{13}\text{C}_{\text{DIC}}$ averaged 13.0 ± 0.8 mM and -0.2 ± 0.3 ‰;
212 POC concentration and $\delta^{13}\text{C}_{\text{POC}}$ averaged 0.05 ± 0.02 mM and -26.1 ± 1.4 ‰. Dissolved oxygen showed a stratified
213 profile with an oxycline layer transitioning from O_2 -saturated to O_2 -depleted conditions between 8 and 14 m depths
214 (Fig. 2). The Chl a concentration showed a large peak at ~ 10 m, reaching 9 $\mu\text{g/L}$ (Fig. 2). The average NH_4^+ and
215 P concentrations were 1.9 and 0.2 μM , respectively. The activity of $\text{CO}_{2(\text{aq})}$ averaged $10^{-4.57}$.

216

217 4.3. Lake Atexcac

218 Bulk DOC had a concentration of ~ 1.1 mM throughout the water column except at 16 and 23 m, where it reached
219 7.7 and 20.8 mM, respectively. The $\delta^{13}\text{C}_{\text{DOC}}$ increased from -20.0 to -8.7 ‰ between 5 and 23 m, decreasing to $-$
220 11.2 ‰ at 30 m. It represented about 16% of the total carbon on average, and 98 % of the organic carbon present
221 in the water column. Total C concentrations and $\delta^{13}\text{C}_{\text{total}}$ are centered around 27.7 mM and -0.6 ‰ with a clear
222 increase to 38.9 mM and decrease to -2.7 ‰ at 23 m, respectively. The $\Delta^{13}\text{C}_{\text{DOC-DIC}}$ values significantly increased
223 from the surface (-20.4 ‰) to the hypolimnion (~ -11.4 ‰). The DOC isotope compositions were strictly and
224 significantly less negative than POC (i.e. enriched in heavy ^{13}C), with $\Delta^{13}\text{C}_{\text{DOC-POC}}$ reaching as much as $+17.9$ ‰
225 at the depth of 23 m (Fig. 4; Table 2). The DIC concentration and $\delta^{13}\text{C}_{\text{DIC}}$ averaged 25.7 ± 0.9 mM and 0.5 ± 0.3 ‰;
226 POC concentration and $\delta^{13}\text{C}_{\text{POC}}$ averaged 0.04 ± 0.02 mM and -27.7 ± 1.1 ‰. Dissolved oxygen showed a stratified
227 profile with an oxycline layer transitioning from O_2 -saturated to O_2 -depleted conditions between 10 and 20 m
228 depths (Fig. 2). Chl a concentration showed a small peak at 16 m, reaching 2 $\mu\text{g/L}$ (Fig. 2). The average NH_4^+ and
229 P concentrations were 2.5 and 0.3 μM , respectively. The activity of $\text{CO}_{2(\text{aq})}$ averaged $10^{-4.27}$.

230

231 4.4. Lake Alchichica

232 Bulk DOC had a concentration of ~ 0.5 mM throughout the water column, except in the hypolimnion, where it
233 reached up to 5.4 mM. The $\delta^{13}\text{C}_{\text{DOC}}$ varied from -29.3 to -25.1 ‰, with maximum values found in the hypolimnion
234 (Fig. 3). The DOC represented about 5 % of the total carbon on average, and 93 % of the organic carbon present
235 in the water column. Total carbon concentration depth profile roughly followed that of DOC, while $\delta^{13}\text{C}_{\text{total}}$ was
236 between -0.2 and 1.6 ‰ throughout the water column, except in the lower part of the hypolimnion, where it
237 decreased to -2.3 ‰ (Table 1). The isotopic difference between DOC and DIC ($\Delta^{13}\text{C}_{\text{DOC-DIC}}$) was slightly smaller
238 in the hypolimnion and was comprised between -26.7 and -30.9 ‰. The DOC isotope compositions were more
239 negative than POC, with $\Delta^{13}\text{C}_{\text{DOC-POC}}$ values between -0.7 and -3.5 ‰ (Fig. 4; Table 2). The DIC concentration
240 and $\delta^{13}\text{C}_{\text{DIC}}$ averaged 34.6 ± 0.6 mM and 1.7 ± 0.2 ‰; POC concentration and $\delta^{13}\text{C}_{\text{POC}}$ averaged 0.01 ± 0.04 and $-$

241 25.6 ± 1.0 ‰. Dissolved oxygen showed a stratified profile with an oxycline layer transitioning from O₂-saturated
 242 to O₂-depleted conditions between ~10 and 20 m depths (Fig. 2). Chl a showed a broad peak between ~ 10 and
 243 30 m, averaging 4 µg/L and with a narrow maximum of 6 µg/L (Fig. 2). The average NH₄⁺ and P concentrations
 244 were 4.3 and 1.5 µM, respectively. The activity of CO_{2(aq)} averaged 10^{-4.53}.

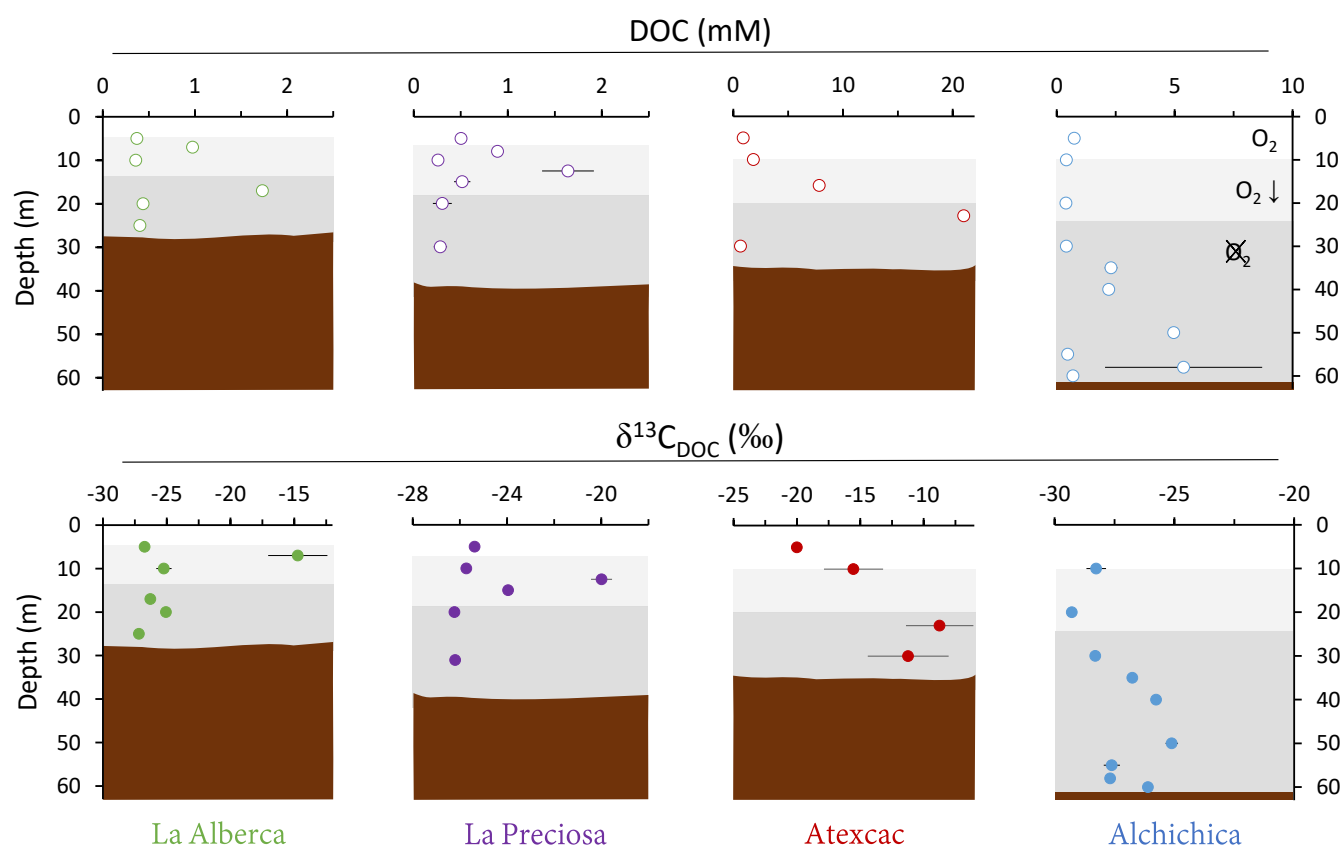
245
 246

247 Table 1

248 Concentration and isotopic composition of dissolved organic carbon (DOC). Total carbon concentration is the
 249 sum of DOC, DIC, and POC reservoirs. For LP 8m, [DIC] was not measured, and the total carbon concentration
 250 was not calculated. The DIC and POC were determined by Havas et al. (2023). The δ¹³C_{Total} is the weighted average
 251 of the three δ¹³C. ND: non-determined.

Lake	Sample	DOC	Total Carbon	δ ¹³ C _{DOC}	δ ¹³ C _{Total}
		mmoles/L		‰	‰
La Alberca de Los Espinosa	Albesp 5m	0.4	7.2	-26.7	-3.9
	Albesp 7m	1.0	8.1	-14.7	-3.9
	Albesp 10m	0.4	7.6	-25.2	-5.1
	Albesp 17m	1.7	9.0	-26.3	-7.9
	Albesp 20m	0.4	8.4	-25.1	-4.5
	Albesp 25m	0.4	9.2	-27.2	-3.2
La Preciosa	LP 5m	0.5	14.0	-25.4	-0.9
	LP 8m	0.9		ND.	ND.
	LP 10m	0.3	13.7	-25.7	-0.4
	LP 12.5m	1.6	13.2	-20.0	-2.8
	LP 15m	0.5	13.9	-24.0	-1.3
	LP 20m	0.3	13.6	-26.2	-1.0
	LP 31m	0.3	13.6	-26.2	-0.9
Atexcac	ATX 5m	0.92	27.4	-20.0	-0.4
	ATX 10m	1.8	28.1	-15.5	-0.7
	ATX 16m	7.8	34.7	ND.	ND.
	ATX 23m	21.0	45.2	-8.7	-3.6
	ATX 30m	0.7	26.4	-11.2	-0.1
Alchichica	AL 5m	0.7	35.8	ND.	ND.
	AL 10m	0.4	33.5	-28.3	1.6
	AL 20m	0.4	35.0	-29.3	1.3
	AL 30m	0.4	35.1	-28.3	1.2
	AL 35m	2.3	37.2	-26.8	-0.2
	AL 40m	2.2	37.0	-25.8	-0.1
	AL 50m	5.0	39.8	-25.1	-1.8
	AL 55m	0.5	35.3	-27.6	1.1
	AL 58m	5.4	40.2	-27.7	-2.3
AL 60m	0.7	35.3	-26.1	1.0	

252
 253
 254



256

257 Figure 3. Vertical profiles of concentration and isotopic composition of dissolved organic carbon (DOC)
 258 throughout the water columns of the studied lakes: La Alberca de los Espinos, La Preciosa, Atexcac, and
 259 Alchichica. Concentration is in mmol/L (mM) and isotopic composition in ‰ vs. VPDB. The white, gray, and dark
 260 gray shading is as in Fig. 2. The brown shading symbolizes the presence of sediment at the bottom of the water
 261 columns (showing the greater water depth in Lake Alchichica).

262

263

264

265

266 5. DISCUSSION

267

268 The four Mexican lakes studied here have a high DOC content but very different profiles and signatures for [DOC]
 269 and $\delta^{13}\text{C}_{\text{DOC}}$ (Fig. 3). Evaporation may increase DOC concentration (Anderson and Stedmon, 2007; Zeyen et al.,
 270 2021), but would not explain the significant intra-lake DOC variability with depth. It is likely marginal because,
 271 in contrast with what was observed for DIC (Havas et al., 2023), there is no correlation between the average DOC
 272 concentration in the Mexican lakes and their salinity ($R^2=0.47$, $p=0.2$ for DOC and $R^2=0.93$, $p=5.8 \cdot 10^{-5}$ for DIC).
 273 In the following discussion, we therefore explore the different patterns of DOC production and fate, in relation to
 274 other environmental and biological variations, and how this can provide information about past DOC-related
 275 perturbations of the C cycle.

276

277 **5.1 Sources and fate of DOC**

278 Due to their endorheic nature, the four lakes receive relatively little allochthonous OM (Alcocer et al., 2014b;
279 Havas et al., 2023). It is therefore possible to focus on DOC-related processes occurring within the water column,
280 particularly on autochthonous DOC primary production. Autochthonous DOC can form through higher-rank OM
281 degradation processes such as sloppy feeding by zooplankton, UV photolysis or bacterial and viral cell lysis
282 (Lampert, 1978; Hessen, 1992; Bade et al., 2007; Thornton, 2014; Brailsford, 2019), as well as passive (leakage)
283 or active (exudation) release by healthy cells (e.g. Baines and Pace, 1991; Hessen and Anderson, 2008; Thornton,
284 2014; Ivanovsky et al., 2020). Generally, this C release (whether “active” or “passive”) tends to be enhanced in
285 nutrient-limited conditions because recently fixed C is in excess compared with other essential nutrients such as
286 N or P (Hessen and Anderson, 2008; Morana et al., 2014; Ivanovsky et al., 2020). For oxygenic phototrophs, this
287 is particularly true under high photosynthesis rates, because photorespiration bolsters the excretion of DOC
288 (Renstrom-Kellner and Bergman, 1989). Oligotrophic conditions also tend to limit heterotrophic bacterial activity
289 and thus preserve DOC stocks (Thornton, 2014; Dittmar, 2015). Both these production and preservation aspects
290 are consistent with the trend of increasing DOC concentrations observed in the lakes, from the less oligotrophic
291 La Alberca and La Preciosa (0.7 mM on average) to the more oligotrophic Alchichica (1.8 mM) and Atexcac
292 (6.5 mM).

293

294 **5.1.1 DOC release by autotrophs**

295 In the four Mexican lakes, DOC concentration profiles exhibit one or several peaks occurring in both oxic and
296 anoxic waters (Fig. 3). In La Alberca and La Preciosa, these peaks correlate with Chl a peaks, but not in the other
297 two lakes. However, in Atexcac, a remarkable DOC peak (Fig. 3) occurs at the same depth as a peak of anoxygenic
298 photosynthesis (Havas et al., 2023). These co-occurrences indicate that a large portion of DOC in these three lakes
299 (at least at these depths) arises from the release of photosynthetic C fixed in excess. Phytoplankton in aerobic
300 conditions generally releases dissolved organic matter by (i) an active “overflow mechanism” (DOM exudation)
301 or (ii) passive diffusion through the cell membranes, but this remains to be shown for anoxygenic organisms. In
302 the first case, DOM is actively released from the cells as a result of C fixation rates higher than growth and
303 molecular synthesis rates (e.g. Baines and Pace, 1991). Hence, DOM exudation depends not only on the nature of
304 primary producers (different taxa may display very different growth rates, photosynthetic efficiency, and exudation
305 mechanisms), but also on environmental factors such as irradiance and nutrient availability (e.g. Otero and
306 Vincenzini, 2003; Morana et al., 2014; Rao et al., 2021). Exudation of DOM may also serve “fitness-promoting
307 purposes” such as storage, defense, or mutualistic goals (Bateson and Ward, 1988; Hessen and Anderson, 2008).
308 In the case of passive diffusion, DOM release also depends on cell permeability and the outward DOC gradient,
309 but is more directly related to the amount of phytoplankton biomass (e.g. Marañón et al., 2004). Thus, any new
310 photosynthate production drives a steady DOM release rate, independent of environmental conditions to some
311 extent (Marañón et al., 2004; Morana et al., 2014). The fact that La Alberca and La Preciosa have lower DOC but
312 Chl a concentrations higher than Atexcac and Alchichica overall, suggests that DOC production does not directly
313 relate to phytoplankton biomass and is not passively released. By contrast, active DOC release is supported by
314 DOC isotope signatures. These tropical Mexican lakes correspond precisely to environmental contexts (high

315 irradiance and oligotrophic freshwater bodies) where DOC exudation has been observed and is predicted (e.g.
316 Baines and Pace, 1991; Morana et al., 2014; Thornton, 2014; Rao et al., 2021).

317 Release of DOC by primary producers can be characterized by the percentage of extracellular release (PER), which
318 corresponds to the fraction of DOC over total (dissolved and particulate) OM primary production (e.g. Thornton
319 et al., 2014). The PER is highly variable and averages about 13% of C biomass over a wide range of environments
320 (e.g. Baines and Pace, 1991; Thornton, 2014). Values as high as 99% have been reported (see Bertilsson and Jones,
321 2003), showing that most of the fixed C can be released in the external aqueous media as DOC. At depths where
322 oxygenic photosynthesis occurs, the DOC over total OC ratio averages approximately 95, 94, 99, and 85 % for La
323 Alberca, La Preciosa, Atexcac, and Alchichica, respectively. Thus, although the PER was not directly measured,
324 and some of the measured DOC may correspond to an older long-term DOC reservoir, the majority of DOC
325 measured could represent a recent phytoplankton exudation.

326 The DOC peaks associated with primary production (mainly photosynthesis) are characterized by very positive
327 $\Delta^{13}\text{C}_{\text{DOC-POC}}$ (from +3 to +18 ‰, Fig. 4). These signatures further support a primary origin of DOC as photosynthate
328 release at these depths, rather than a secondary origin by OM degradation. Bacterial heterotrophy would generate
329 smaller and rather negative $\Delta^{13}\text{C}_{\text{DOC-POC}}$ (section 5.1.2. and references therein) and cell lysis or zooplankton sloppy
330 feeding would also produce $\delta^{13}\text{C}_{\text{DOC}}$ close to $\delta^{13}\text{C}_{\text{POC}}$ values. Photo-degradation is unlikely to proceed at these
331 depths and would not generate such positive fractionations (Chomicki, 2009). A switch from $\text{CO}_{2(\text{aq})}$ to HCO_3^- as
332 an inorganic C source (which differ by 10‰, e.g. Mook et al., 1974) would not adequately explain the deviation
333 between $\delta^{13}\text{C}_{\text{POC}}$ and $\delta^{13}\text{C}_{\text{DOC}}$. The isotopic enrichment of DOC molecules relative to POC must therefore have a
334 different origin.

335 The ^{13}C -enriched DOC could originate from photosynthetic organisms using a different C-fixation pathway,
336 inducing a smaller isotopic fractionation (provided that these organisms contributed predominantly to the DOC
337 rather than to the POC fraction). In La Alberca and Atexcac, anoxygenic phototrophic bacteria may release large
338 amounts of DOC, especially under nutrient-limiting conditions (Ivanovsky et al., 2020). Unlike cyanobacteria or
339 purple sulfur bacteria (PSB, anoxygenic phototrophs belonging to the Proteobacteria), which use the Calvin-
340 Benson-Bassham pathway (CBB), green sulfur bacteria (GSB; another group of anoxygenic phototrophs belonging
341 to the Chlorobi), use the reductive citric acid cycle or reverse tricarboxylic-TCA cycle, which tends to induce
342 smaller isotopic fractionations (between ~ 3–13 ‰, Hayes, 2001). The DOC isotope signatures recorded in the
343 hypolimnion of La Alberca ($\epsilon_{\text{DOC-CO}_2} \approx -13.5 \pm 2$ ‰) agree well with fractionations found for this type of organism
344 in laboratory cultures and in stratified water bodies (Posth et al., 2017). By contrast, $\epsilon_{\text{DOC-CO}_2}$ signatures in the
345 hypolimnion of Atexcac are higher ($\epsilon_{\text{DOC-CO}_2} \approx 0$ ‰), and thus cannot be explained by the use of the reductive
346 citric acid cycle C fixation pathway. Consistently, GSB were identified in La Alberca but not in Atexcac (Havas
347 et al., 2023).

348 Phytoplankton blooms may specifically release isotopically heavy organic molecules. Carbohydrates could be
349 preferentially released under nutrient-limiting conditions as they are devoid of N and P (Bertilsson and Jones,
350 2003; Wetz and Wheeler, 2007; Thornton, 2014). Carbohydrates typically have a ^{13}C -enriched (heavy) isotopic
351 composition (Blair et al., 1985; Jiao et al., 2010; Close and Henderson, 2020). Considering the isotopic mass

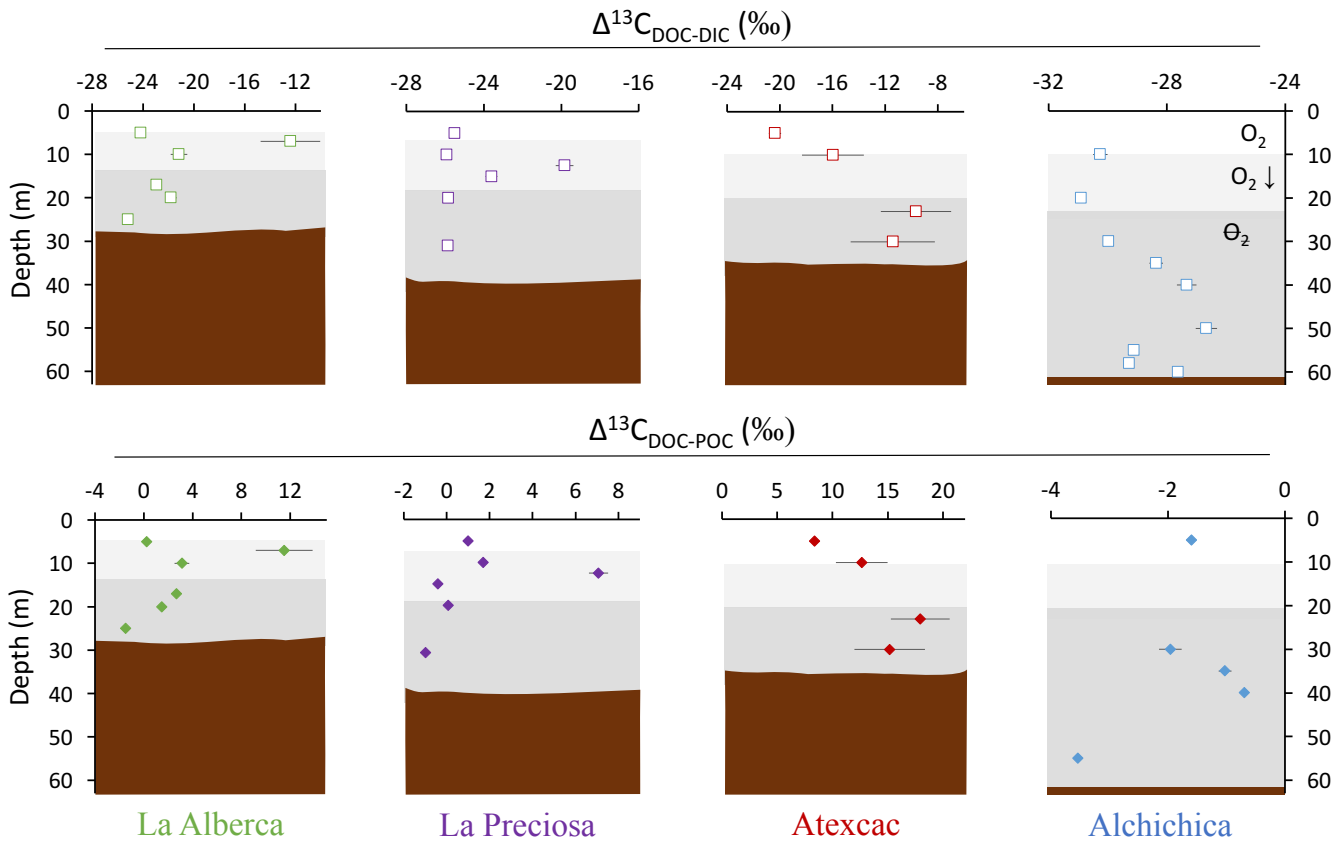
352 balance of cell specific organic compounds, this molecular hypothesis is insufficient to explain the full range of
353 $\Delta^{13}\text{C}_{\text{DOC-POC}}$ variations measured in La Alberca and Atexcac (Hayes, 2001).

354 Alternatively, such enrichments require that DOC and DIC first accumulate in the cells. If DOC molecules were
355 released as soon as they were produced, their isotopic composition would tend towards that of the biomass (i.e.
356 $\delta^{13}\text{C}_{\text{POC}}$, within the range of molecule-specific isotopic compositions), which is not the case. If DIC could freely
357 exchange between inner and outer cell media, maximum “carboxylation-limited” fractionation (between ~ 18 and
358 30 ‰ depending on RuBisCO form, Thomas et al., 2019) would be expressed in all synthesized organic molecules,
359 as represented in Fig. 5a (e.g. O’Leary, 1988; Descolas-Gros and Fontungne, 1990; Fry, 1996). This is also
360 inconsistent with the DOC isotopic signatures (see $\epsilon_{\text{DOC-CO}_2}$ in Table. 2).

361 Under the environmental conditions of the lakes studied (i.e. low CO_2 relative to HCO_3^- , local planktonic
362 competition for CO_2 , and low nutrient availability), the activation of an intracellular DIC-concentrating mechanism
363 (DIC-CM) is expected (Beardall et al., 1982; Burns and Beardall, 1987; Fogel and Cifuentes, 1993; Badger et al.,
364 1998; Iñiguez et al., 2020). This mechanism is particularly relevant in oligotrophic aqueous media (Beardall et al.,
365 1982), where CO_2 diffusion is slower than in the air (O’Leary, 1988; Fogel and Cifuentes, 1993; Iñiguez et al.,
366 2020). A DIC-CM has been proposed to reduce the efflux of DIC from the cells back to the extracellular solution.
367 This internal DIC is eventually converted into organic biomass, thereby drawing the cell isotopic composition
368 closer to that of $\delta^{13}\text{C}_{\text{DIC}}$ (Fig. 5; Beardall et al., 1982; Fogel and Cifuentes, 1993; Werne and Hollander, 2004). As
369 a conceptual model, we suggest that the activation of a DIC-CM could preserve a large $\Delta^{13}\text{C}_{\text{POC-DIC}}$, while
370 generating an apparent fractionation between the DOC and POC molecules. The initially fixed OC would be
371 discriminated against the heavy C isotopes, and incorporated into the cellular biomass (Fig. 5c, ‘ t_i ’). In turn,
372 following the overflow mechanism scenario, high photosynthetic rates (due to high irradiance and temperature,
373 and high DIC despite low CO_2) coupled with low population growth rates and organic molecule synthesis (due to
374 limited abundances of P, N, and Fe), would result in the exudation of excess organic molecules with heavy $\delta^{13}\text{C}_{\text{DOC}}$,
375 as they are synthesized from residual internal DIC, which progressively becomes ^{13}C -enriched (Fig. 5c, ‘ t_{ii} ’). This
376 process could explain the formation of DOC with $\delta^{13}\text{C}$ very close to DIC/ CO_2 signatures as observed in Lake
377 Atexcac. This suggests that oligotrophic conditions could be a determinant factor in the generation of significantly
378 heavy $\delta^{13}\text{C}_{\text{DOC}}$, even more so if they are coupled to high irradiance. This also demonstrates that considerable
379 isotopic variability can exist between these two organic C reservoirs.

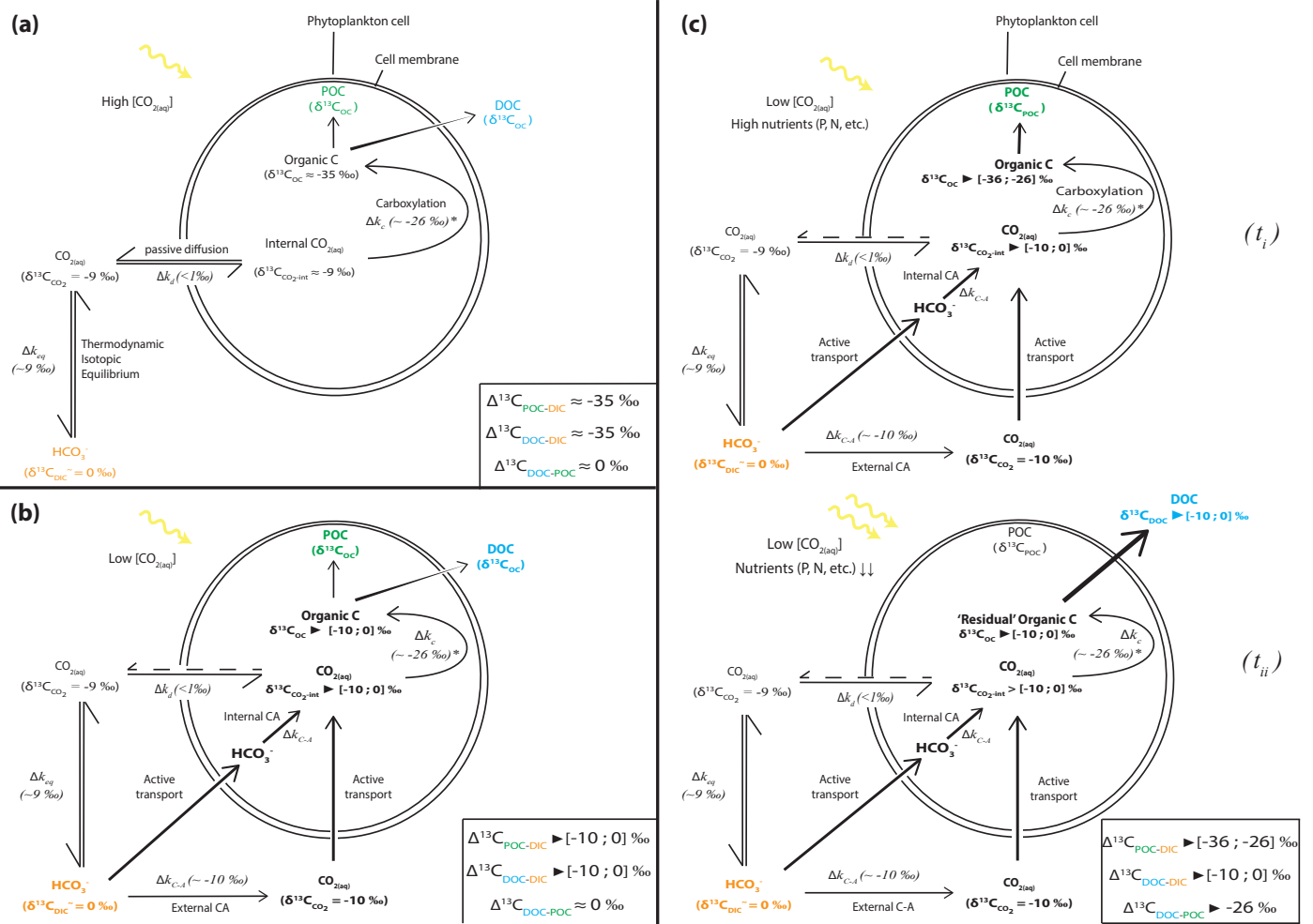
380
381 In summary, the unusual [DOC] and $\delta^{13}\text{C}_{\text{DOC}}$ profiles in La Alberca, La Preciosa and Atexcac could be interpreted
382 as mainly reflecting a prominent exudation of autochthonous C, fixed in excess by oxygenic and/or anoxygenic
383 phototrophs in nutrient-poor and high-irradiance conditions. The striking ^{13}C -rich signatures of these exudates are
384 interpreted as reflecting either the activation of a DIC-CM by oxygenic and/or anoxygenic phototrophs or the
385 fixation of C *via* the reductive citric acid cycle. We propose a conceptual model involving the DIC-CM, whereby
386 oligotrophic and high irradiance contexts can lead to high $\delta^{13}\text{C}_{\text{DOC}}$ compared to both $\delta^{13}\text{C}_{\text{DIC}}$ and $\delta^{13}\text{C}_{\text{POC}}$.

387
388
389
390



391
 392 Figure 4. Vertical profiles of the difference in $\delta^{13}\text{C}$ values of DOC and DIC (top) as well as DOC and POC (bottom)
 393 throughout the water columns of the four lakes (all expressed as $\Delta^{13}\text{C}$ in ‰ vs. VPDB). POC and DIC data used in
 394 these calculations are from Havas et al. (2023). In Alchichica, $\delta^{13}\text{C}_{\text{DOC}}$ was not measured at 5 m and its value at 10
 395 m was used in this calculation of $\Delta^{13}\text{C}_{\text{DOC-POC}}$. The white, gray, and dark gray shading is as in Fig. 2. The brown
 396 shading symbolizes the presence of sediment at the bottom of the water columns.

397
 398
 399
 400
 401
 402
 403
 404
 405
 406
 407
 408
 409



411

412 Figure 5. Schematic view of phytoplankton cells during autotrophic C fixation through different C supply
 413 strategies and associated apparent isotopic fractionation between DIC and POC/DOC and between DOC and POC.
 414 (a) Case where $[CO_{2(aq)}]$ is high enough to allow for a DIC supply by passive $CO_{2(aq)}$ diffusion through the cell
 415 membrane and $CO_{2(aq)}$ is at equilibrium with other DIC species. Isotopic fractionation is maximum (minimum
 416 $\delta^{13}C_{OC}$) because C fixation is limited by the carboxylation step. DOC is released following an in- to outward cell
 417 concentration gradient and has a similar composition to POC. (b) “Classic” view of C isotopic cycling resulting
 418 from active DIC transport within the cell because of low ambient $[CO_{2(aq)}]$ (through a DIC-CM). Carbonic anhydrase
 419 (CA) catalyzes the conversion between HCO_3^- and $CO_{2(aq)}$ inside or outside the cell with isotopic fractionation close
 420 to equilibrium fractionation ($\sim 10\text{‰}$). While inward passive $CO_{2(aq)}$ diffusion can still occur, the DIC-CM activation
 421 reduces the reverse diffusion, resulting in internal $CO_{2(aq)}$ isotopic composition approaching that of the incoming
 422 DIC (depending on the fraction of internal $CO_{2(aq)}$ leaving the cell). Acting as a “closed-system”, most of the
 423 internal DIC is fixed as OC, and minimum isotopic fractionation is expressed for both POC and DOC. (c) Proposed
 424 model for C isotopic fractionation with active DIC transport including isotopic discrimination between POC and
 425 DOC. (t_i) Initially fixed C is isotopically depleted and incorporates the cell’s biomass as long as there are sufficient
 426 nutrients to enable the synthesis of “complex” organic molecules. (t_{ii}) In low nutrient conditions, but with high
 427 photosynthetic activity – subsequently fixed C is released out of the cell as DOC following the “overflow”
 428 hypothesis and inherits heavier isotopic compositions from the residual internal DIC. This leads to distinct POC
 429 and DOC isotopic signatures, with small fractionation between DOC and DIC, the amplitude of which will depend
 430 on the rate of CO_2 backward diffusion, and the biomass C (POC) to released C (DOC) ratio.

431

432 5.1.2 OM partial degradation and DOC accumulation: the case of Lake Alchichica

433 From the previous discussion, it appears that the environmental conditions of the Mexican lakes favor substantial
434 phytoplankton production of DOC. Alcocer et al. (2014a) proposed that an early spring cyanobacterial bloom in
435 Lake Alchichica may favor the production of DOC in the epilimnion. However, at the time of sampling, the DOC
436 reservoir in this lake was not correlated with any sizeable autotrophic activity at any depth. The large epilimnetic
437 Chl a peak did not correlate with any changes in [DOC] or $\delta^{13}\text{C}_{\text{DOC}}$ (Fig. 3). Compared with the other lakes, the
438 geochemical conditions in which Chl a was produced in Alchichica may have been incompatible with the
439 activation of a DIC-CM and significant DOC exudation. Alchichica had similar $[\text{CO}_{2(\text{aq})}]$ to La Preciosa, but higher
440 P and NH_4^+ concentrations (Havas et al., 2023); La Alberca had higher P concentrations, but similar $[\text{NH}_4^+]$ and
441 lower $[\text{CO}_{2(\text{aq})}]$. In contrast with measurements from 2013 (Alcocer et al., 2014a), we found a large increase in
442 DOC in the middle of the anoxic hypolimnion of Alchichica, which did not correspond to any change in the DIC
443 reservoir, unlike that observed for La Preciosa at 12.5 m and Atexcac at 23 m (Havas et al., 2023). At these depths,
444 photosynthetic active radiation (PAR) is below 0.1% in Alchichica during the stratified season (Macek et al.,
445 2020), which might not be sufficient to trigger major anoxygenic phytoplankton DOC release.

446 The DOC reservoir in Alchichica is characterized by a $\delta^{13}\text{C}_{\text{DOC}}$ (and $\Delta^{13}\text{C}_{\text{DOC-DIC}}$) lower than in the other lakes,
447 systematically showing ^{13}C -depleted signatures relative to POC (i.e. $\delta^{13}\text{C}_{\text{DOC}} < \delta^{13}\text{C}_{\text{POC}}$; Fig. 4). Thus, if the DOC
448 increase in the hypolimnion of Alchichica resulted from the release of photosynthetic OC, as in some of the other
449 lakes, it was not associated with the same C isotope fractionation (e.g. if anoxygenic phototrophs did not
450 concentrate intracellular DIC, cf. Fig. 5a). Some PSB have been identified but they only become abundant toward
451 the end of the stratification (from July/August to December/January; Alcántara-Hernández et al., 2022; Iniesto et
452 al., 2022).

453 Alternatively, the hypolimnetic DOC increase in Lake Alchichica may reflect the preservation and accumulation
454 of DOM over the years, consistent with the higher [DOC] measured in 2019 than in the previous years (Alcocer
455 et al., 2014a). While alteration of the DOC reservoir by UV-photolysis would induce positive isotopic fractionation
456 (Chomicki, 2009), the slightly negative $\Delta^{13}\text{C}_{\text{DOC-POC}}$ signatures support the possibility of DOC being mainly a
457 recalcitrant residue of primary OM degradation by heterotrophic organisms (Alcocer et al., 2014a). The
458 preferential consumption of labile ^{13}C -enriched molecules by heterotrophic bacteria would leave the residual OM
459 with more negative isotopic signatures (Williams and Gordon, 1970; Lehmann et al., 2002; Close and Henderson,
460 2020). The DIC and POM data were also consistent with heterotrophic activity from the surface to the hypolimnion
461 of Alchichica, by recording complementary decreasing and increasing $\delta^{13}\text{C}$, respectively, and a decreasing C:N
462 ratio (Havas et al., 2023). Degradation by heterotrophic bacteria leaves more recalcitrant DOM in the water
463 column, which tends to accumulate over longer periods of time (Ogawa et al., 2001; Jiao et al., 2010; Kawasaki et
464 al., 2013). The DOM content is a balance between production by autotrophs and consumption by heterotrophs,
465 especially in environments where both types of organisms compete for low-concentration nutrients (Dittmar,
466 2015). If the DOC in Alchichica represents a long-term reservoir, its presence might favor the development of
467 bacterial populations. A shift of the cyanobacterial DOC from the epilimnion toward the hypolimnion of
468 Alchichica was described at the end of the spring (Alcocer et al., 2014a; 2022). Thus, part of the hypolimnetic
469 DOC in Alchichica may originate from a phytoplankton release, as observed in the other lakes, but it was already
470 partially degraded by heterotrophic bacteria at the time we sampled it. The deeper and darker anoxic waters of

471 Alchichica could help to better preserve this DOC from intense microbial and light degradation, hence allowing
 472 its accumulation over time.

473 In conclusion, the DOC reservoir in Alchichica (notably in the hypolimnion) more likely represents an older, more
 474 evolved DOM pool. The time required for its accumulation and long-term stability has not yet been evaluated.

475

476

477

478 Table 2

479 Isotopic fractionation between DOC and DIC, and DOC and POC, where $\Delta^{13}\text{C}_{x-y} = \delta^{13}\text{C}_x - \delta^{13}\text{C}_y$ is the apparent
 480 fractionation and ϵ is computed as the actual metabolic isotopic discrimination between CO_2 and DOC. In
 481 Alchichica, $\delta^{13}\text{C}_{\text{DOC}}$ was not measured at 5 m, and its value at 10 m was used in this calculation of $\Delta^{13}\text{C}_{\text{DOC-POC}}$. The
 482 full chemistry at depths 35 and 58 m was not determined, thus the calculation of $\delta^{13}\text{C}_{\text{CO}_2}$ for these samples is
 483 based on the composition of samples above and below. Isotopic data for DIC, POC, and CO_2 are from Havas et al.
 484 (2023).

Lake	Sample	$\Delta^{13}\text{C}_{\text{DOC-DIC}}$	$\Delta^{13}\text{C}_{\text{DOC-POC}}$	$\epsilon_{\text{DOC-CO}_2}$
		‰		‰
La Alberca de Los Espinos	Albesp 5m	-24.2	0.2	-14.8
	Albesp 7m	-12.4	11.5	-3.0
	Albesp 10m	-21.2	3.1	-11.6
	Albesp 17m	-22.9	2.7	-13.1
	Albesp 20m	-21.8	1.5	-12.2
	Albesp 25m	-25.2	-1.5	-15.9
La Preciosa	LP 5m	-25.5	1.0	-15.7
	LP 10m	-25.9	1.7	-16.0
	LP 12.5m	-19.8	7.1	-9.8
	LP 15m	-23.6	-0.4	-13.5
	LP 20m	-25.8	0.1	-15.7
	LP 31m	-25.8	-1.0	-15.7
Atexcac	ATX 5m	-20.4	8.4	-10.6
	ATX 10m	-16.0	12.6	-6.1
	ATX 23m	-9.7	17.9	0.6
	ATX 30m	-11.4	15.2	-1.2
Alchichica	AL 5m	ND.	-1.6	
	AL 10m	-30.3		-20.1
	AL 20m	-30.9		-20.5
	AL 30m	-30.0	-2.0	-19.5
	AL 35m	-28.4	-1.0	-17.9
	AL 40m	-27.3	-0.7	-16.8
	AL 50m	-26.7		-16.2
	AL 55m	-29.1	-3.5	-18.7
	AL 58m	-29.3		-18.8
AL 60m	-27.6		-17.1	

485

486

487 **5.2 DOC analysis provides deeper insights into planktonic cell functioning and water column C cycle**
488 **dynamics than POC or DIC analyses**

489 The depth profiles of DOC concentration and isotope composition differ significantly from those of POC. Notably
490 in La Preciosa, the photosynthetic DOC production (+1.5 mM) at the Chl a peak depth matches the decrease in
491 DIC (- 2 mM), while there was no change in [POC] or $\delta^{13}\text{C}_{\text{POC}}$ (Havas et al., 2023). Just below, at 15 m depth,
492 $\delta^{13}\text{C}_{\text{POC}}$ exhibited a marked increase (+3.6 ‰) interpreted as reflecting heterotrophic activity (Havas et al., 2023).
493 It is likely explained by the production of DOC with heavier isotope compositions between 12.5 and 15 m depth,
494 and its consumption by heterotrophic organisms (as seen with $\Delta^{13}\text{C}_{\text{DOC-POC}} \approx 0$). In La Alberca, the peaks of
495 oxygenic and anoxygenic photosynthesis clearly stand out from DOC concentrations (+ 0.5/1.5 mM), but not from
496 POC concentrations (+ <0.03 mM), while the DIC geochemical signatures reflected the influence of OC
497 respiration, sediment-associated methanogenesis, and possible volcanic degassing at the bottom of the lake (Havas
498 et al., 2023). In Atexcac, anoxygenic photosynthesis is clearly evidenced by [DOC] and $\delta^{13}\text{C}_{\text{DOC}}$ data (see 5.1.1),
499 but is not recorded by the POC reservoir (a decrease of 0.03 mM at this depth) and not as distinctively by the DIC
500 reservoir (a decrease of ~ 2 mM; Havas et al., 2023). It implies that recently fixed OC is quickly released out of
501 the cells as DOC, transferring most C from DIC to DOC, rather than POC, which is therefore an incomplete archive
502 of the biogeochemical reactions occurring in water columns. The isotopic analysis of DIC, and by extension of
503 authigenic carbonates, especially in alkaline-buffered waters, might not be sensitive enough to faithfully record all
504 environmental and biological changes.

505 The $\delta^{13}\text{C}_{\text{DOC}}$ recorded in La Alberca, La Preciosa, and Atexcac present peculiar heavy signatures, which provide
506 strong constraints on planktons intra-cellular functioning and their use of C. These signatures may arise from the
507 activation of a DIC-CM or from a specific metabolism or C-fixation pathway. By contrast, the use of a DIC-CM
508 is poorly captured by $\delta^{13}\text{C}_{\text{POC}}$, although recognition of active DIC uptake has often been based on this signal (by
509 reduced isotopic fractionation with DIC; e.g. Beardall et al., 1982; Erez et al., 1998; Riebesell et al., 2000). Most
510 interestingly, intra-cellular amorphous Ca-carbonates (iACC) are formed in some of the cyanobacteria from
511 Alchichica microbialites, possibly due to supersaturated intra-cell media following active DIC uptake through a
512 DIC-CM (Couradeau et al., 2012; Benzerara et al., 2014). While the link between DIC-CM and iACC still needs
513 to be demonstrated (Benzerara et al., 2014), the active use of DIC-CMs in Mexican lakes is independently
514 supported by the DOC isotopic signature.

515 In summary, the analysis of DOC concentrations and isotope compositions showed that most of the autochthonous
516 C fixation ends up in the DOC reservoir, thus highlighting important features of the lakes and their C cycle that
517 were not evidenced by POC and DIC analyses alone, notably the activation of a DIC-CM and a better description
518 of the planktonic diversity. In the future, it will be interesting to couple the present analyses with deeper molecular
519 and compound-specific isotopic analyses of DOM (Wagner et al., 2020).

520

521 **5.3 Implications for the hypothesis of a large DOC reservoir controlling past carbon cycling**

522 In these Mexican lakes, the DOC concentrations (from 0.6 to 6.5 mM on average) are between 14 and 160 times
523 higher than the POC concentrations. The DOC represents from 5 to 16% of the total C measured in the four lakes.
524 In comparison, it remains under 0.3 mM in large-scale anoxic basins such as the Black Sea (Ducklow et al., 2007).

525 In the modern ocean, DOC is also the main organic pool but its concentration rarely exceeds 0.08 mM (Hansell,
526 2013). Thus, the DOC pools of these lakes is much larger than in the modern ocean and can be used to draw
527 comparisons with studies invoking past occurrences of oceanic carbon cycles dominated by vast DOC reservoirs
528 (e.g. Rothman et al., 2003; Sexton et al., 2011).

529

530 **5.3.1 Eocene carbon isotope excursions (CIEs)**

531 Ventilation/oxidation cycles of a large deep ocean DOC reservoir have been inferred to explain carbonate isotopic
532 records of successive warming events through the Eocene (Sexton et al., 2011). In this scenario, the release of
533 carbon dioxide into the ocean/atmosphere system following DOC oxidation would trigger both the precipitation
534 of low $\delta^{13}\text{C}$ carbonates and an increase of the atmospheric greenhouse gas content. The size of this DOC reservoir
535 should have been at least 1600 PgC (about twice the size of the modern ocean DOC reservoir) to account for a 2–
536 4°C increase in deep ocean temperatures (Sexton et al., 2011). However, the main counter-argument to this
537 hypothesis is that the buildup of such a DOC reservoir at modern DOC production rates implies sustained deep
538 ocean anoxia over several hundred thousand years, while independent geochemical proxies do not support the
539 persistence of such anoxic conditions (Rigwell and Arndt, 2015). Our study suggests, albeit at a different scale,
540 that this kinetic argument may be weak. In these Mexican lakes, the lowest recorded [DOC] is 260 μM (Table 1),
541 which is about 6 times the deep modern ocean concentration ($\sim 45 \mu\text{M}$; Hansell, 2013). Yet the entire water
542 columns of these lakes down to the surficial sediments are seasonally mixed with di-oxygen, showing that high
543 [DOC] (notably in Alchichica, which likely harbors a “long-term” DOC reservoir) can be achieved despite frequent
544 oxidative conditions. The oxidation of only half of the DOC in the lakes would generate average $\delta^{13}\text{C}_{\text{DIC}}$ deviations
545 between -0.6 and -1 ‰, corresponding to the C isotope excursion magnitudes described by Sexton et al. (2011).

546 Similarly, deep anoxic waters in the Black Sea hold about 3 times the amount of DOC found in the modern deep
547 open ocean (Ducklow et al., 2007; Sexton et al., 2011; Dittmar, 2015). In the Black Sea and in the Mexican lakes,
548 low nutrient availability may limit sulfate-reduction despite high sulfate and labile organic matter concentrations,
549 thus favoring DOM preservation and accumulation (Dittmar, 2015 and references therein). Margolin et al. (2016)
550 argued that substantial DOM is maintained in the Black Sea by large terrigenous inputs only. Our study attests the
551 possibility for “autochthonous systems” to reach DOC concentrations well above what is found in the Black Sea,
552 without requiring terrigenous inputs. Therefore, it supports the hypothesis that the buildup of a large DOC reservoir
553 may have influenced the carbonate isotopic record of Eocene warming events. Nonetheless, it remains to be proven
554 how this could apply to larger oceanic-type basins, with more variable environmental conditions (e.g. tropical vs.
555 polar latitudes), greater diversity of eukaryotic heterotrophs (in Phanerozoic oceans), and more active water
556 currents and ventilation processes. A better characterization of the molecular composition of DOM in the Mexican
557 lakes will help to understand how it can accumulate over time and refine the suggested analogy with Phanerozoic
558 CIEs. Furthermore, investigating the paleo-ecology and -geography of the CIE time period will also help to
559 constrain the potential applicability of a large DOC hypothesis (Sexton et al., 2011).

560

561

562

563 5.3.2 Neoproterozoic carbon isotope excursions (CIEs)

564 The presence of a large oceanic DOC reservoir has also been used to account for the Neoproterozoic C isotope
565 record, where carbonates show $\delta^{13}\text{C}$ negative excursions of more than 10‰ over tens of Ma (Rothman et al., 2003;
566 Fike et al., 2006; Swanson-Hysell et al., 2010; Tziperman et al., 2011). Once again, this hypothesis has been
567 questioned because of (i) the oversized DOC reservoir (10 times the contemporaneous DIC, i.e., 10^2 to 10^3 times
568 that of modern DOC) and (ii) the amount of oxidants required to generate such a sustained DOC oxidation process
569 (see Ridgwell and Arndt, 2015). Recent studies offered potential explanations for this latter issue showing that
570 pulses of continental weathering and an associated increase of sulfate supply would have provided sufficient
571 oxidant (Shields et al., 2019; Chen et al., 2022), while lateral heterogeneity of the carbonate geochemical signatures
572 – with a restricted record of the CIEs on the continental shelves – would require lower amounts of oxidant (Li et
573 al., 2017; Shi et al., 2017).

574 Critically though, direct evidence for the existence of such high oceanic DOC levels in the past remains scarce (Li
575 et al., 2017), although multiple studies have built on the Neoproterozoic large DOC scenario (e.g. Sperling et al.,
576 2011; Cañadas et al., 2022). Purported high oceanic DOC concentrations during the Ediacaran period have been
577 estimated from the Ge/Si ratio of diagenetic chert nodules (Xing et al., 2022) but they reflect the sediments
578 porewater geochemistry and remain difficult to directly relate to the ocean water itself. Besides, some modeling
579 approaches have suggested that DOC abundance in the past Earth’s oceans could not have markedly differed from
580 today’s values (Fakraee et al., 2021).

581 Modern analogous systems such as the Black Sea or Mexican lakes studied here support the possibility of greater
582 DOC accumulation in anoxic waters (Ducklow et al., 2007), but only to levels substantially lower than those
583 required to account for the Neoproterozoic CIEs (minimum concentrations estimated between 25 and 100 mM;
584 Ridgwell and Arndt, 2015). One could argue that the development of larger DOC pools in the three Mexican lakes
585 from the SOB is hindered by relatively large sulfate reservoirs (especially in Alchichica ~10 mM). However, we
586 notice that La Alberca does not show a larger DOC reservoir despite having the lowest oxidant availability (both
587 oxygen- and sulfate-free at depth) and being the only one of the four lakes to present isotopic signatures associated
588 with methanogenesis (Havas et al., 2023). Furthermore, the Mexican lakes are seasonally oxidized, which could
589 consume part of their DOC reservoir. However, the Black Sea is permanently stratified and shows even lower
590 [DOC], suggesting that DOC production might be the primary control on DOC concentration over DOC oxidation.
591 The processes of DOC production and accumulation in the Neoproterozoic ocean could have been less efficient
592 than today (Fakraee et al. 2021). Nonetheless, an important limit to the analogy between modern analogues and
593 the Precambrian oceans is the difference in time over which DOC could have accumulated in both environments
594 (Ridgwell and Arndt, 2015). One could expect the formation of such a large autochthonous DOC reservoir to
595 increase the ocean inorganic C isotope composition, by mass balance. However, from $\delta^{13}\text{C}_{\text{Carb}}$ data compilation
596 (e.g. Fike et al., 2006; Saltzman and Thomas, 2012; Li et al., 2017), we see that there are no positive increases of
597 $\delta^{13}\text{C}_{\text{Carb}}$ at the magnitude of the negative CIEs tens to hundreds of million years before the Neoproterozoic CIEs.
598 Thus, even if the “oxidant paradox” may have found satisfactory explanations, the origin of the massive DOC
599 reservoir required to generate these excursions still remains to be elucidated (Jiang et al., 2010; Lu et al., 2013; Li
600 et al., 2017).

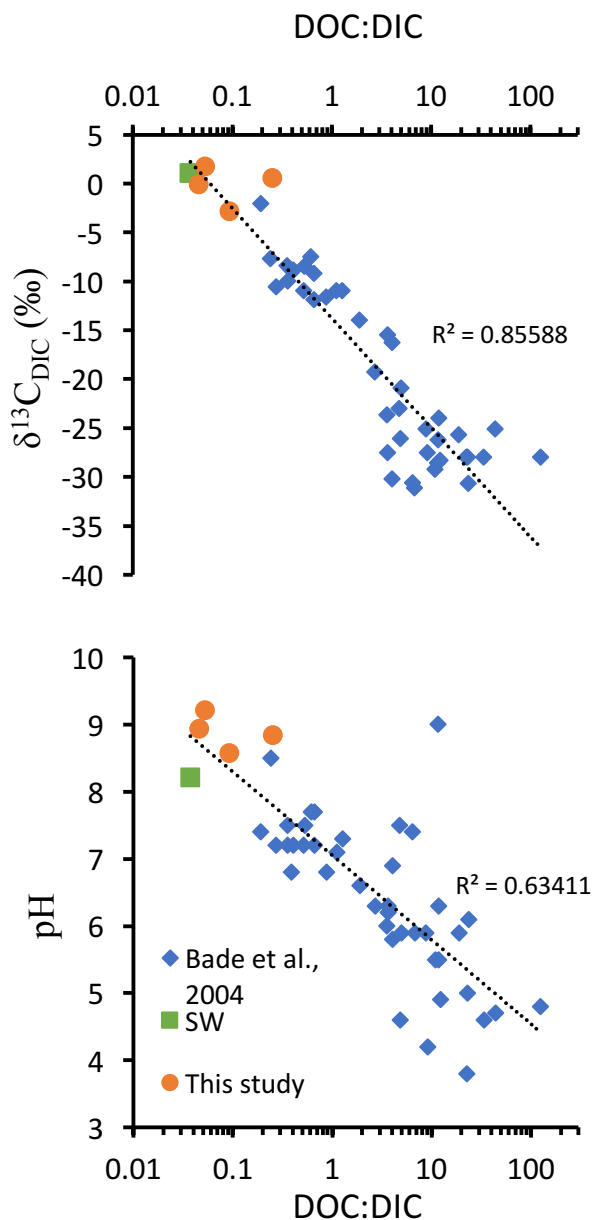


Figure 6. DOC:DIC ratios, pH and $\delta^{13}\text{C}_{\text{DIC}}$ values from different lakes compiled from Bade et al. (2004) and the four Mexican lakes from Havas et al. (2023), as well as modern surface ocean values (from Kroopnick, 1985; Zeebe and Wolf-Gladrow, 2009 and Hansell, 2013).

Top: $\delta^{13}\text{C}_{\text{DIC}}$ as a function of DOC:DIC ratio represented with a logarithmic abscissa scale and logarithmic trend line which combines the three datasets.

Bottom: pH as a function of DOC:DIC ratio, with a logarithmic abscissa scale and logarithmic trend line which combines the three datasets.

624

625 In the alkaline lakes studied, oxidation of the DOC reservoir would generate a maximum $\delta^{13}\text{C}_{\text{DIC}}$ deviation of -
 626 2 ‰, in La Alberca de los Espinos, which has the lowest alkalinity. The other lakes $\delta^{13}\text{C}_{\text{DIC}}$ are less impacted,
 627 notably because they are largely buffered by high DIC content (Havas et al., 2023). Bade et al. (2004) showed that
 628 modern low alkalinity/low pH lakes generally show more negative $\delta^{13}\text{C}_{\text{DIC}}$ (down to ~ -30 ‰), partly due to a
 629 higher responsiveness of the $\delta^{13}\text{C}_{\text{DIC}}$ to remineralization of OM and especially DOC. Compiling our data with
 630 those of Bade et al. (2004), we consistently show a clear negative trend of $\delta^{13}\text{C}_{\text{DIC}}$ with an increasing DOC:DIC
 631 ratio over a broad range of lacustrine DOC and DIC concentrations (Fig. 6). This trend also matches modern ocean
 632 values (Fig. 6). These observations are consistent with the inference that systems where $\text{DOC:DIC} \gg 1$ should
 633 drive $\delta^{13}\text{C}_{\text{DIC}}$ to very negative values (Rothman et al., 2003). However, in modern environments, the biomass is
 634 largely influenced by aerobic heterotrophs and high DOC:DIC waters usually lean toward acidic pHs (Fig. 6; Bade
 635 et al., 2004), at which carbonate precipitation is prevented. Instead, in anoxic waters, remineralization of OM
 636 through sulfate- or iron-reduction generates alkalinity (e.g. Tziperman et al., 2011). Hence, environmental

637 conditions where DOC:DIC \gg 1 might be inconsistent with large carbonate deposits unless they are associated
638 with anaerobic remineralization. This further supports the hypothesis that negative $\delta^{13}\text{C}_{\text{carb}}$ excursions of the
639 Ediacaran were triggered by continental sulfate addition to the ocean (Li et al., 2017; Shields et al., 2019; Chen et
640 al., 2022), but following the oxidation of DOC by anaerobic (e.g. sulfate reduction) rather than aerobic (e.g. by
641 free oxygen) pathways. At the same time, additional DOC inputs (e.g. terrigenous) might be necessary to reach
642 the required high DOC conditions allowing the Neoproterozoic CIEs. This echoes previous suggestions of
643 “Neoproterozoic greening”, referring to a phase of biological land colonization, although evidence for this
644 phenomenon currently remains equivocal (Lenton and Daines, 2017). While a concomitant supply of sulfate and
645 DOC *via* rivers may cause – at least – a partial oxidation of DOC, it would still result in a ^{13}C -depleted source of
646 alkalinity to the coastal environments.

647 The inferences from Fig. 6 also foster the scenario proposed by Tziperman et al. (2011) where the anaerobic
648 respiration of a large DOM production leads to the sequestration of newly produced C in carbonates – with very
649 negative $\delta^{13}\text{C}$ – and thereby to the drawdown of atmospheric pCO_2 and the initiation of Cryogenian glaciations.
650 We therefore suggest that the climatic feedbacks associated with the negative Neoproterozoic CIEs have been
651 controlled by the total amount and balance between different DOC sources (autochthonous vs. allochthonous), and
652 different oxidation pathways (e.g. via O_2 vs. SO_4^{2-}).

653 In summary, Neoproterozoic carbonate carbon isotope excursions likely require DOC and DIC pools to be spatially
654 decoupled (e.g. through terrestrial DOM inputs), which suggests that DOC was not necessarily larger than DIC in
655 the entire ocean. The analogues studied here further support that the Neoproterozoic CIEs recorded in carbonates
656 should have occurred following DOC oxidation through anaerobic rather than aerobic pathways.

657

658 **6. CONCLUSIONS AND SUMMARY**

659 Based on its concentration and isotopic signatures, we characterized the nature and role of the DOC reservoir
660 within the C cycle of four stratified alkaline crater lakes, in comparison with previously described DIC and POC
661 data. Despite similar contexts, the DOC reservoirs of the four lakes show considerable variability, driven by
662 environmental and ecological differences, as summarized below:

- 663 - The DOC is the largest OC reservoir in the water column of the studied lakes (> 90%). Its concentration
664 and isotopic composition provide novel information about the C cycle of these stratified water bodies. In
665 each of the four lakes, diverse photosynthetic planktonic communities release greater or smaller amounts
666 of DOC, depending strongly on environmental factors such as nutrient and DIC availability, and transfer
667 most of the inorganic C to DOC rather than POC.
- 668 - This process is marked by very heavy and distinct isotopic signatures of DOC compared with POC. They
669 reflect different metabolism/C fixation pathways and/or the activity of a DIC-CM coupled with an
670 overflow mechanism (i.e. DOM exudation), which could be active for both oxygenic and anoxygenic
671 phototrophs, and for which we propose a novel isotopic model of cell carbon cycling, integrating DOC
672 molecules.
- 673 - The DOC reservoir in one of the lakes was not characterized by this release process, but rather by partial
674 degradation and accumulation in anoxic waters, associated with more negative isotopic signatures.

675 - Our results bring further constraints on the environmental conditions under which autochthonous DOM
676 can accumulate in anoxic water bodies, providing boundary conditions to the large DOC reservoir
677 scenarios. This study of modern redox-stratified analogues supports the idea that a large oceanic DOC
678 reservoir may have generated the record of successive C isotope excursions during the Eocene. Our study
679 suggests, however, that the Neoproterozoic large DOC hypothesis and its record in carbonates as negative
680 CIEs would only have been possible if external DOC sources largely contributed, and if DOC oxidation
681 occurred *via* anaerobic pathways.

682

683 **Data Availability**

684 Data are publicly accessible at: <https://doi.org/10.26022/IEDA/112943>.

685

686 **Author Contributions**

687 RH and CT designed the study in a project directed by PLG, KB and CT. CT, MI, DJ, DM, RT, PLG and KB
688 collected the samples on the field. RH carried out the measurements for C data; DJ the physico-chemical parameter
689 probe measurements and EM provided data for trace and major elements. RH and CT analyzed the data. RH wrote
690 the manuscript with important contributions of all co-authors.

691

692 **Competing Interests**

693 The authors declare that they have no conflict of interest.

694

695 **Disclaimer**

696

697 **Acknowledgements**

698 This work was supported by Agence Nationale de la Recherche (France; ANR Microbialites, grant number ANR-
699 18-CE02-0013-02). The authors thank Anne-Lise Santoni, Elodie Cognard, Théophile Cocquerez and the GISMO
700 platform (Biogéosciences, University Bourgogne Franche-Comté, UMR CNRS 6282, France). We thank Céline
701 Liorzou and Bleuenn Guéguen for the analyses at the Pôle Spectrométrie Océan (Laboratoire Géo-Océan, Brest,
702 France) and Laure Cordier for ion chromatography analyses at IPGP (France). We thank Nelly Assayag and Pierre
703 Cadeau for their help on the AP 2003 at IPGP. We warmly thank Carmela Chateau-Smith for improving the syntax
704 and clarity of the manuscript.

705

706 **References**

707 Alcántara-Hernández, R.J., Macek, M., Torres-Huesca, J., Arellano-Posadas, J., Valdespino-Castillo,
708 P.M.: Bacterioplankton, in: Alcocer, J. (Ed.), Lake Alchichica Limnology: The Uniqueness of a Tropical
709 Maar Lake. Springer International Publishing, Cham, pp. 183–196, [https://doi.org/10.1007/978-3-
710 030-79096-7_11](https://doi.org/10.1007/978-3-030-79096-7_11), 2022.

711 Alcocer, J., Guzmán-Arias, A., Oseguera, L.A., Escobar, E.: Dinámica del carbono orgánico disuelto y
712 particulado asociados al florecimiento de *Nodularia spumigena* en un lago tropical oligotrófico,
713 Programa Mexicano del Carbono, 404-410, 2014a.

714 Alcocer, J., Ruiz-Fernández, A.C., Escobar, E., Pérez-Bernal, L.H., Oseguera, L.A., Ardiles-Gloria, V.:
715 Deposition, burial and sequestration of carbon in an oligotrophic, tropical lake, *J. Limnol.*, 73, 223-
716 235, DOI: 10.4081/jlimnol.2014.783, 2014b.

717 Anderson, N.J., Stedmon, C.A.: The effect of evapoconcentration on dissolved organic carbon
718 concentration and quality in lakes of SW Greenland, *Freshw. Biol.*, 52, 280–289,
719 <https://doi.org/10.1111/j.1365-2427.2006.01688.x>, 2007.

720 Armienta, M.A., Vilaclara, G., De la Cruz-Reyna, S., Ramos, S., Cenicerros, N., Cruz, O., Aguayo, A.,
721 Arcega-Cabrera, F.: Water chemistry of lakes related to active and inactive Mexican volcanoes, *J.*
722 *Volcanol. Geotherm. Res.*, 178, 249–258, <https://doi.org/10.1016/j.jvolgeores.2008.06.019>, 2008.

723 Bade, D.L., Carpenter, S.R., Cole, J.J., Hanson, P.C., Hesslein, R.H.: Controls of $\delta^{13}\text{C}$ -DIC in lakes:
724 Geochemistry, lake metabolism, and morphometry, *Limnol. Oceanogr.*, 49, 1160–1172,
725 <https://doi.org/10.4319/lo.2004.49.4.1160>, 2004.

726 Bade, D.L., Carpenter, S.R., Cole, J.J., Pace, M.L., Kritzberg, E., Van de Bogert, M.C., Cory, R.M.,
727 McKnight, D.M.: Sources and fates of dissolved organic carbon in lakes as determined by whole-lake
728 carbon isotope additions, *Biogeochemistry*, 84, 115–129, [https://doi.org/10.1007/s10533-006-9013-](https://doi.org/10.1007/s10533-006-9013-y)
729 [y](https://doi.org/10.1007/s10533-006-9013-y), 2007.

730 Badger, M.R., Andrews, T.J., Whitney, S.M., Ludwig, M., Yellowlees, D.C., Leggat, W., Price, G.D.: The
731 diversity and coevolution of Rubisco, plastids, pyrenoids, and chloroplast-based CO_2 -concentrating
732 mechanisms in algae, *Can. J. Botany*, 76, 1052-1071, <https://doi.org/10.1139/b98-074>, 1998.

733 Baines, S.B., Pace, M.L.: The production of dissolved organic matter by phytoplankton and its
734 importance to bacteria: Patterns across marine and freshwater systems, *Limnol. Oceanogr.*, 36,
735 1078–1090, <https://doi.org/10.4319/lo.1991.36.6.1078>, 1991.

736 Barber, A., Sirois, M., Chaillou, G., Gélinas, Y.: Stable isotope analysis of dissolved organic carbon in
737 Canada's eastern coastal waters: Stable isotope analysis of DOC, *Limnol. Oceanogr.*, 62, S71–S84.
738 <https://doi.org/10.1002/lno.10666>, 2017.

739 Bateson, M.M., Ward, D.M.: Photoexcretion and Fate of Glycolate in a Hot Spring Cyanobacterial
740 Mat, *Appl. Environ. Microbiol.*, 54, 1738–1743, <https://doi.org/10.1128/aem.54.7.1738-1743>, 1988.

741 Beardall, J., Griffiths, H., Raven, J.A.: Carbon Isotope Discrimination and the CO_2 Accumulating
742 Mechanism in *Chlorella emersonii*, *J. Exp. Bot.*, 33, 729–737, <https://doi.org/10.1093/jxb/33.4.729>,
743 1982.

744 Beaupré, S.R.: The Carbon Isotopic Composition of Marine DOC, in: *Biogeochemistry of Marine*
745 *Dissolved Organic Matter*, Elsevier, pp. 335–368, [https://doi.org/10.1016/B978-0-12-405940-](https://doi.org/10.1016/B978-0-12-405940-5.00006-6)
746 [5.00006-6](https://doi.org/10.1016/B978-0-12-405940-5.00006-6), 2015.

747 Benzerara, K., Skouri-Panet, F., Li, J., Féraud, C., Gugger, M., Laurent, T., Couradeau, E., Ragon, M.,
748 Cosmidis, J., Menguy, N., Margaret-Oliver, I., Tavera, R., López-García, P., Moreira, D.: Intracellular
749 Ca-carbonate biomineralization is widespread in cyanobacteria, *Proc. Natl. Acad. Sci.*, 111, 10933–
750 10938, <https://doi.org/10.1073/pnas.1403510111>, 2014.

751 Bertilsson, S., Jones, J.B.: Supply of Dissolved Organic Matter to Aquatic Ecosystems: Autochthonous
752 Sources, in: Findlay, S.E.G., Sinsabaugh, R.L. (Eds.), *Aquatic Ecosystems, Aquatic Ecology*, Academic
753 Press, Burlington, pp. 3–24, <https://doi.org/10.1016/B978-012256371-3/50002-0>, 2003.

754 Blair, N., Leu, A., Muñoz, E., Olsen, J., Kwong, E., Des Marais, D.: Carbon isotopic fractionation in
755 heterotrophic microbial metabolism, *Appl. Environ. Microbiol.*, 50, 996–1001,
756 <https://doi.org/10.1128/aem.50.4.996-1001.1985>, 1985.

757 Brailsford, F.L.: Dissolved organic matter (DOM) in freshwater ecosystems, Bangor University (UK),
758 2019.

759 Burns, B.D., Beardall, J.: Utilization of inorganic carbon by marine microalgae, *J. Exp. Mar. Biol. Ecol.*,
760 107, 75–86, [https://doi.org/10.1016/0022-0981\(87\)90125-0](https://doi.org/10.1016/0022-0981(87)90125-0), 1987.

761 Cadeau, P., Jézéquel, D., Leboulanger, C., Fouilland, E., Le Floc’h, E., Chaduteau, C., Milesi, V.,
762 Guélard, J., Sarazin, G., Katz, A., d’Amore, S., Bernard, C., Ader, M.: Carbon isotope evidence for large
763 methane emissions to the Proterozoic atmosphere, *Sci. Rep.*, 10, 18186,
764 <https://doi.org/10.1038/s41598-020-75100-x>, 2020.

765 Cañadas, F., Papineau, D., Leng, M.J., Li, C.: Extensive primary production promoted the recovery of
766 the Ediacaran Shuram excursion, *Nat. Commun.*, 13, 148, [https://doi.org/10.1038/s41467-021-](https://doi.org/10.1038/s41467-021-27812-5)
767 [27812-5](https://doi.org/10.1038/s41467-021-27812-5), 2022.

768 Carlson, C.A., Hansell, D.A.: DOM Sources, Sinks, Reactivity, and Budgets, in: *Biogeochemistry of*
769 *Marine Dissolved Organic Matter*, Elsevier, pp. 65–126, [https://doi.org/10.1016/B978-0-12-405940-](https://doi.org/10.1016/B978-0-12-405940-5.00003-0)
770 [5.00003-0](https://doi.org/10.1016/B978-0-12-405940-5.00003-0), 2015.

771 Carrasco-Núñez, G., Ort, M.H., Romero, C.: Evolution and hydrological conditions of a maar volcano
772 (Atexcac crater, Eastern Mexico), *J. Volcanol. Geotherm. Res.*, 159, 179–197,
773 <https://doi.org/10.1016/j.jvolgeores.2006.07.001>, 2007.

774 Cawley, K.M., Ding, Y., Fourqrean, J., Jaffé, R.: Characterising the sources and fate of dissolved
775 organic matter in Shark Bay, Australia: a preliminary study using optical properties and stable carbon
776 isotopes, *Mar. Freshw. Res.*, 63, 1098, <https://doi.org/10.1071/MF12028>, 2012.

777 Chako Tchamabé, B., Carrasco-Núñez, G., Miggins, D.P., Németh, K.: Late Pleistocene to Holocene
778 activity of Alchichica maar volcano, eastern Trans-Mexican Volcanic Belt, *J. South Am. Earth Sci.*, 97,
779 102404, <https://doi.org/10.1016/j.jsames.2019.102404>, 2020.

780 Chen, B., Hu, C., Mills, B.J.W., He, T., Andersen, M.B., Chen, X., Liu, P., Lu, M., Newton, R.J., Poulton,
781 S.W., Shields, G.A., Zhu, M.: A short-lived oxidation event during the early Ediacaran and delayed
782 oxygenation of the Proterozoic ocean, *Earth Planet. Sci. Lett.*, 577, 117274,
783 <https://doi.org/10.1016/j.epsl.2021.117274>, 2022.

784 Chomicki, K.: The use of stable carbon and oxygen isotopes to examine the fate of dissolved organic
785 matter in two small, oligotrophic Canadian Shield lakes, University of Waterloo (Canada), 2009.

786 Close, H.G., Henderson, L.C.: Open-Ocean Minima in $\delta^{13}\text{C}$ Values of Particulate Organic Carbon in the
787 Lower Euphotic Zone, *Front. Mar. Sci.*, 7, 540165, <https://doi.org/10.3389/fmars.2020.540165>, 2020.

788 Couradeau, E., Benzerara, K., Gérard, E., Moreira, D., Bernard, S., Brown, G.E., López-García, P.: An
789 Early-Branching Microbialite Cyanobacterium Forms Intracellular Carbonates, *Science*, 336, 459–462,
790 <https://doi.org/10.1126/science.1216171>, 2012.

791 Crowe, S.A., Katsev, S., Leslie, K., Sturm, A., Magen, C., Nomosatryo, S., Pack, M.A., Kessler, J.D.,
792 Reeburgh, W.S., Roberts, J.A., González, L., Douglas Haffner, G., Mucci, A., Sundby, B., Fowle, D.A.:
793 The methane cycle in ferruginous Lake Matano: Methane cycle in ferruginous Lake Matano,
794 *Geobiology*, 9, 61–78, <https://doi.org/10.1111/j.1472-4669.2010.00257.x>, 2011.

795 Descolas-Gros, C., Fontungne, M.: Stable carbon isotope fractionation by marine phytoplankton
796 during photosynthesis, *Plant Cell Environ.*, 13, 207–218, [https://doi.org/10.1111/j.1365-](https://doi.org/10.1111/j.1365-3040.1990.tb01305.x)
797 3040.1990.tb01305.x, 1990.

798 Dittmar, T.: Reasons Behind the Long-Term Stability of Dissolved Organic Matter, in: *Biogeochemistry*
799 *of Marine Dissolved Organic Matter*, Elsevier, pp. 369–388, [https://doi.org/10.1016/B978-0-12-](https://doi.org/10.1016/B978-0-12-405940-5.00007-8)
800 405940-5.00007-8, 2015.

801 Ducklow, H.W., Hansell, D.A., Morgan, J.A.: Dissolved organic carbon and nitrogen in the Western
802 Black Sea, *Mar. Chem.*, 105, 140–150, <https://doi.org/10.1016/j.marchem.2007.01.015>, 2007.

803 Erez, J., Bouevitch, A., Kaplan, A.: Carbon isotope fractionation by photosynthetic aquatic
804 microorganisms: experiments with *Synechococcus* PCC7942, and a simple carbon flux model, *Can. J.*
805 *Bot.*, 76, 1109–1118, <https://doi.org/10.1139/b98-067>, 1998.

806 Fakhraee, M., Tarhan, L.G., Planavsky, N.J., Reinhard, C.T.: A largely invariant marine dissolved
807 organic carbon reservoir across Earth’s history, *Proc. Natl. Acad. Sci.*, 118, e2103511118,
808 <https://doi.org/10.1073/pnas.2103511118>, 2021.

809 Ferrari, L., Orozco-Esquivel, T., Manea, V., Manea, M.: The dynamic history of the Trans-Mexican
810 Volcanic Belt and the Mexico subduction zone, *Tectonophysics*, 522–523, 122–149,
811 <https://doi.org/10.1016/j.tecto.2011.09.018>, 2012.

812 Fike, D.A., Grotzinger, J.P., Pratt, L.M., Summons, R.E.: Oxidation of the Ediacaran Ocean, *Nature*,
813 444, 744–747, <https://doi.org/10.1038/nature05345>, 2006.

814 Fogel, M.L., Cifuentes, L.A.: Isotope Fractionation during Primary Production, in: Engel, M.H., Macko,
815 S.A. (Eds.), *Organic Geochemistry, Topics in Geobiology*. Springer US, Boston, MA, pp. 73–98,
816 https://doi.org/10.1007/978-1-4615-2890-6_3, 1993.

817 Fry, B.: $^{13}\text{C}/^{12}\text{C}$ fractionation by marine diatoms, *Mar. Eco. Prog. Ser.*, 134, pp.283-294,
818 doi:10.3354/meps134283, 1996.

819 Hansell, D.A.: Recalcitrant Dissolved Organic Carbon Fractions, *Annu. Rev. Mar. Sci.*, 5, 421–445,
820 <https://doi.org/10.1146/annurev-marine-120710-100757>, 2013.

821 Havas, R., Thomazo, C., Iniesto, M., Jézéquel, D., Moreira, D., Tavera, R., Caumartin, J., Muller, E.,
822 López-García, P., and Benzerara, K.: A comparative isotopic study of the biogeochemical cycle of
823 carbon in modern stratified lakes: the hidden role of DOC, *Biogeosciences*,
824 <https://doi.org/10.5194/bg-2022-149>, 2022.

825 Havig, J.R., McCormick, M.L., Hamilton, T.L., Kump, L.R.: The behavior of biologically important trace
826 elements across the oxic/euxinic transition of meromictic Fayetteville Green Lake, New York, USA,
827 *Geochim. Cosmochim. Acta*, 165, 389–406, <https://doi.org/10.1016/j.gca.2015.06.024>, 2015.

828 Havig, J.R., Hamilton, T.L., McCormick, M., McClure, B., Sowers, T., Wegter, B., Kump, L.R.: Water
829 column and sediment stable carbon isotope biogeochemistry of permanently redox-stratified
830 Fayetteville Green Lake, New York, U.S.A., *Limnol. Oceanogr.*, 63, 570–587,
831 <https://doi.org/10.1002/lno.10649>, 2018.

832 Hayes, J.M.: Fractionation of Carbon and Hydrogen Isotopes in Biosynthetic Processes*, *Rev. Mineral.*
833 *Geochem.*, 43, 225–277, <https://doi.org/10.2138/gsrmg.43.1.225>, 2001.

834 Hessen, D.O.: Dissolved organic carbon in a humic lake: effects on bacterial production and
835 respiration, in: Salonen, K., Kairesalo, T., Jones, R.I. (Eds.), *Dissolved Organic Matter in Lacustrine*
836 *Ecosystems: Energy Source and System Regulator*, *Developments in Hydrobiology*. Springer
837 Netherlands, Dordrecht, pp. 115–123, https://doi.org/10.1007/978-94-011-2474-4_9, 1992.

838 Hessen, D.O., Anderson, T.R.: Excess carbon in aquatic organisms and ecosystems: Physiological,
839 ecological, and evolutionary implications, *Limnol. Oceanogr.*, 53, 1685–1696,
840 <https://doi.org/10.4319/lo.2008.53.4.1685>, 2008.

841 Iniesto, M., Moreira, D., Benzerara, K., Reboul, G., Bertolino, P., Tavera, R., López-García, P.:
842 Planktonic microbial communities from microbialite-bearing lakes sampled along a salinity-alkalinity
843 gradient, *Limnol. Oceanogr.*, Ino.12233, <https://doi.org/10.1002/Ino.12233>, 2022.

844 Iñiguez, C., Capó-Bauçà, S., Niinemets, Ü., Stoll, H., Aguiló-Nicolau, P., Galmés, J.: Evolutionary trends
845 in RuBisCO kinetics and their co-evolution with CO₂ concentrating mechanisms, *Plant J.*, 101, 897–
846 918, <https://doi.org/10.1111/tpj.14643>, 2020.

847 Ivanovsky, R.N., Lebedeva, N.V., Keppen, O.I., Chudnovskaya, A.V.: Release of Photosynthetically
848 Fixed Carbon as Dissolved Organic Matter by Anoxygenic Phototrophic Bacteria, *Microbiology*, 89,
849 28–34, <https://doi.org/10.1134/S0026261720010075>, 2020.

850 Jiang, G., Wang, X., Shi, X., Zhang, S., Xiao, S., Dong, J.: Organic carbon isotope constraints on the
851 dissolved organic carbon (DOC) reservoir at the Cryogenian–Ediacaran transition, *Earth Planet. Sci.*
852 *Lett.*, 299, 159–168, <https://doi.org/10.1016/j.epsl.2010.08.031>, 2010.

853 Jiang, G., Wang, X., Shi, X., Xiao, S., Zhang, S., Dong, J.: The origin of decoupled carbonate and organic
854 carbon isotope signatures in the early Cambrian (ca. 542–520Ma) Yangtze platform, *Earth Planet. Sci.*
855 *Lett.*, 317–318, 96–110, <https://doi.org/10.1016/j.epsl.2011.11.018>, 2012.

856 Jiao, N., Herndl, G.J., Hansell, D.A., Benner, R., Kattner, G., Wilhelm, S.W., Kirchman, D.L., Weinbauer,
857 M.G., Luo, T., Chen, F., Azam, F.: Microbial production of recalcitrant dissolved organic matter: long-
858 term carbon storage in the global ocean, *Nat. Rev. Microbiol.*, 8, 593–599.
859 <https://doi.org/10.1038/nrmicro2386>, 2010.

860 Kaplan, L.A., Wiegner, T.N., Newbold, J.D., Ostrom, P.H., Gandhi, H.: Untangling the complex issue of
861 dissolved organic carbon uptake: a stable isotope approach, *Freshw. Biol.*, 53, 855–864,
862 <https://doi.org/10.1111/j.1365-2427.2007.01941.x>, 2008.

863 Kawasaki, N., Komatsu, K., Kohzu, A., Tomioka, N., Shinohara, R., Satou, T., Watanabe, F.N., Tada, Y.,
864 Hamasaki, K., Kushairi, M.R.M., Imai, A.: Bacterial Contribution to Dissolved Organic Matter in
865 Eutrophic Lake Kasumigaura, Japan, *Appl. Environ. Microbiol.*, 79, 7160–7168,
866 <https://doi.org/10.1128/AEM.01504-13>, 2013.

867 Kroopnick, P.M.: The distribution of ¹³C of ΣCO₂ in the world oceans, *Deep Sea Research Part A.*
868 *Oceanographic Research Papers*, 32, 57–84, [https://doi.org/10.1016/0198-0149\(85\)90017-2](https://doi.org/10.1016/0198-0149(85)90017-2), 1985.

869 Kuntz, L.B., Laakso, T.A., Schrag, D.P., Crowe, S.A.: Modeling the carbon cycle in Lake Matano,
870 *Geobiology*, 13, 454–461, <https://doi.org/10.1111/gbi.12141>, 2015.

871 Lampert, W.: Release of dissolved organic carbon by grazing zooplankton, *Limnol. Oceanogr.*, 23,
872 831–834, <https://doi.org/10.4319/lo.1978.23.4.0831>, 1978.

873 Lehmann, M.F., Bernasconi, S.M., Barbieri, A., McKenzie, J.A.: Preservation of organic matter and
874 alteration of its carbon and nitrogen isotope composition during simulated and in situ early

875 sedimentary diagenesis, *Geochim. Cosmochim. Ac.*, 66, 3573–3584, <https://doi.org/10.1016/S0016->
876 7037(02)00968-7, 2002.

877 Lenton, T.M., Daines, S.J.: The effects of marine eukaryote evolution on phosphorus, carbon and
878 oxygen cycling across the Proterozoic–Phanerozoic transition, *Emerg. Top. Life Sci.*, 2, 267–278,
879 <https://doi.org/10.1042/ETLS20170156>, 2018.

880 Lenton, T.M., Daines, S.J.: Matworld – the biogeochemical effects of early life on land, *New Phytol.*,
881 215, 531–537, <https://doi.org/10.1111/nph.14338>, 2017.

882 Li, C., Hardisty, D.S., Luo, G., Huang, J., Algeo, T.J., Cheng, M., Shi, W., An, Z., Tong, J., Xie, S., Jiao, N.,
883 Lyons, T.W.: Uncovering the spatial heterogeneity of Ediacaran carbon cycling, *Geobiology*, 15, 211–
884 224, <https://doi.org/10.1111/gbi.12222>, 2017.

885 Lu, M., Zhu, M., Zhang, J., Shields-Zhou, G., Li, G., Zhao, F., Zhao, X., Zhao, M.: The DOUNCE event at
886 the top of the Ediacaran Doushantuo Formation, South China: Broad stratigraphic occurrence and
887 non-diagenetic origin, *Precambrian Res.*, 225, 86–109,
888 <https://doi.org/10.1016/j.precamres.2011.10.018>, 2013.

889 Lugo, A., Alcocer, J., Sanchez, M.R., Escobar, E.: Trophic status of tropical lakes indicated by littoral
890 protozoan assemblages, *Internationale Vereinigung für theoretische und angewandte Limnologie:*
891 *Verhandlungen*, 25:1, 4441-443, <https://doi.org/10.1080/03680770.1992.11900159>, 1993.

892 Lyons, T.W., Reinhard, C.T., Planavsky, N.J.: The rise of oxygen in Earth’s early ocean and atmosphere,
893 *Nature*, 506, 307–315, <https://doi.org/10.1038/nature13068>, 2014.

894 Macek, M., Medina, X.S., Picazo, A., Peštová, D., Reyes, F.B., Hernández, J.R.M., Alcocer, J., Ibarra,
895 M.M., Camacho, A.: *Spirostomum teres*: A Long Term Study of an Anoxic-Hypolimnion Population
896 Feeding upon Photosynthesizing Microorganisms, *Acta Protozool*, 59, 13–38.
897 <https://doi.org/10.4467/16890027AP.20.002.12158>, 2020.

898 Marañón, E., Cermeño, P., Fernández, E., Rodríguez, J., Zabala, L.: Significance and mechanisms of
899 photosynthetic production of dissolved organic carbon in a coastal eutrophic ecosystem, *Limnol.*
900 *Oceanogr.*, 49, 1652–1666, <https://doi.org/10.4319/lo.2004.49.5.1652>, 2004.

901 Margolin, A.R., Gerringa, L.J.A., Hansell, D.A., Rijkenberg, M.J.A.: Net removal of dissolved organic
902 carbon in the anoxic waters of the Black Sea, *Mar. Chem.*, 183, 13–24,
903 <https://doi.org/10.1016/j.marchem.2016.05.003>, 2016.

904 Morana, C., Sarmiento, H., Descy, J.-P., Gasol, J.M., Borges, A.V., Bouillon, S., Darchambeau, F.:
905 Production of dissolved organic matter by phytoplankton and its uptake by heterotrophic
906 prokaryotes in large tropical lakes, *Limnol. Oceanogr.*, 59, 1364–1375,
907 <https://doi.org/10.4319/lo.2014.59.4.1364>, 2014.

908 Organization for Economic Cooperation and Development (OECD), Vollenweider, R.A., Kerekes, J.:
909 *Eutrophication of waters. Monitoring, assessment and control*: Paris, pp. 154, 1982.

910 Ogawa, H., Amagai, Y., Koike, I., Kaiser, K., Benner, R.: Production of Refractory Dissolved Organic
911 Matter by Bacteria, *Science*, 292, 917–920, <https://doi.org/10.1126/science.1057627>, 2001.

912 O’Leary, M.H.: Carbon Isotopes in Photosynthesis, *BioScience*, 38, 328–336,
913 <https://doi.org/10.2307/1310735>, 1988

914 Otero, A., Vincenzini, M.: Extracellular polysaccharide synthesis by Nostoc strains as affected by N
915 source and light intensity, *J. Biotechnol.*, 102, 143–152, [https://doi.org/10.1016/S0168-](https://doi.org/10.1016/S0168-1656(03)00022-1)
916 1656(03)00022-1, 2003.

917 Peltier, W.R., Liu, Y., Crowley, J.W.: Snowball Earth prevention by dissolved organic carbon
918 remineralization, *Nature*, 450, 813–818, <https://doi.org/10.1038/nature06354>, 2007.

919 Petrash, D.A., Steenbergen, I.M., Valero, A., Meador, T.B., Pačes, T., Thomazo, C.: Aqueous system-
920 level processes and prokaryote assemblages in the ferruginous and sulfate-rich bottom waters of a
921 post-mining lake, *Biogeosciences*, 19, 1723–1751, <https://doi.org/10.5194/bg-19-1723-2022>, 2022.

922 Posth, N.R., Bristow, L.A., Cox, R.P., Habicht, K.S., Danza, F., Tonolla, M., Frigaard, N. -U., Canfield,
923 D.E.: Carbon isotope fractionation by anoxygenic phototrophic bacteria in euxinic Lake Cadagno,
924 *Geobiology*, 15, 798–816, <https://doi.org/10.1111/gbi.12254>, 2017.

925 Rao, D.N., Chopra, M., Rajula, G.R., Durgadevi, D.S.L., Sarma, V.V.S.S.: Release of significant fraction
926 of primary production as dissolved organic carbon in the Bay of Bengal, *Deep Sea Res. Part Oceanogr.*
927 *Res. Pap.*, 168, 103445, <https://doi.org/10.1016/j.dsr.2020.103445>, 2021.

928 Renstrom-Kellner, E., Bergman, B.: Glycolate metabolism in cyanobacteria. III. Nitrogen controls
929 excretion and metabolism of glycolate in *Anabaena cylindrica*, *Physiol. Plant.*, 77, 46–51,
930 <https://doi.org/10.1111/j.1399-3054.1989.tb05976.x>, 1989.

931 Repeta, D.J., Aluwihare, L.I.: Radiocarbon analysis of neutral sugars in high-molecular-weight
932 dissolved organic carbon: Implications for organic carbon cycling, *Limnol. Oceanogr.*, 51, 1045–1053,
933 <https://doi.org/10.4319/lo.2006.51.2.1045>, 2006.

934 Ridgwell, A., Arndt, S.: Chapter 1 - Why Dissolved Organics Matter: DOC in Ancient Oceans and Past
935 Climate Change, in: Hansell, D.A., Carlson, C.A. (Eds.), *Biogeochemistry of Marine Dissolved Organic*
936 *Matter (Second Edition)*. Academic Press, Boston, pp. 1–20, [https://doi.org/10.1016/B978-0-12-](https://doi.org/10.1016/B978-0-12-405940-5.00001-7)
937 405940-5.00001-7, 2015.

938 Riebesell, U., Burkhardt, S., Dauelsberg, A., Kroon, B.: Carbon isotope fractionation by a marine
939 diatom: dependence on the growth-rate-limiting resource, *Mar. Ecol. Prog. Ser.*, 193, 295–303,
940 <https://doi.org/10.3354/meps193295>, 2000.

941 Rothman, D.H., Hayes, J.M., Summons, R.E.: Dynamics of the Neoproterozoic carbon cycle. *Proc. Natl.*
942 *Acad. Sci.*, 100, 8124–8129, <https://doi.org/10.1073/pnas.0832439100>, 2003.

943 Saini, J.S., Hassler, C., Cable, R., Fourquez, M., Danza, F., Roman, S., Tonolla, M., Storelli, N., Jacquet,
944 S., Zdobnov, E.M., Duhaime, M.B.: Microbial loop of a Proterozoic ocean analogue, *bioRxiv*, 2021-08,
945 <https://doi.org/10.1101/2021.08.17.456685>, 2021.

946 Saltzman, M.R., Thomas, E.: Carbon Isotope Stratigraphy, in: *The Geologic Time Scale*, Elsevier, pp.
947 207–232, <https://doi.org/10.1016/B978-0-444-59425-9.00011-1>, 2012.

948 Santinelli, C., Follett, C., Retelletti Brogi, S., Xu, L., Repeta, D.: Carbon isotope measurements reveal
949 unexpected cycling of dissolved organic matter in the deep Mediterranean Sea, *Mar. Chem.*, 177,
950 267–277. <https://doi.org/10.1016/j.marchem.2015.06.018>, 2015.

951 Satkoski, A.M., Beukes, N.J., Li, W., Beard, B.L., Johnson, C.M.: A redox-stratified ocean 3.2 billion
952 years ago, *Earth Planet. Sci. Lett.*, 430, 43–53. <https://doi.org/10.1016/j.epsl.2015.08.007>, 2015.

953 Schiff, S.L., Tsuji, J.M., Wu, L., Venkiteswaran, J.J., Molot, L.A., Elgood, R.J., Paterson, M.J., Neufeld,
954 J.D.: Millions of Boreal Shield Lakes can be used to Probe Archaean Ocean Biogeochemistry, *Sci. Rep.*,
955 7, 46708, <https://doi.org/10.1038/srep46708>, 2017.

956 Sexton, P.F., Norris, R.D., Wilson, P.A., Pälike, H., Westerhold, T., Röhl, U., Bolton, C.T., Gibbs, S.:
957 Eocene global warming events driven by ventilation of oceanic dissolved organic carbon, *Nature*, 471,
958 349–352, <https://doi.org/10.1038/nature09826>, 2011.

959 Shi, W., Li, C., Algeo, T.J.: Quantitative model evaluation of organic carbon oxidation hypotheses for
960 the Ediacaran Shuram carbon isotopic excursion, *Sci. China Earth Sci.*, 60, 2118–2127,
961 <https://doi.org/10.1007/s11430-017-9137-1>, 2017.

962 Shields, G.A., Mills, B.J.W., Zhu, M., Raub, T.D., Daines, S.J., Lenton, T.M.: Unique Neoproterozoic
963 carbon isotope excursions sustained by coupled evaporite dissolution and pyrite burial, *Nat. Geosci.*,
964 12, 823–827, <https://doi.org/10.1038/s41561-019-0434-3>, 2019.

965 Siebe, C., Guilbaud, M.-N., Salinas, S., Chédeville-Monzo, C.: Eruption of Alberca de los Espinos tuff
966 cone causes transgression of Zacapu lake ca. 25,000 yr BP in Michoacán, México, Presented at the IAS
967 4IMC Conference, Auckland, New Zealand, pp. 74–75, 2012.

968 Siebe, C., Guilbaud, M.-N., Salinas, S., Kshirsagar, P., Chevrel, M.O., Jiménez, A.H., Godínez, L.:
969 Monogenetic volcanism of the Michoacán-Guanajuato Volcanic Field: Maar craters of the Zacapu
970 basin and domes, shields, and scoria cones of the Tarascan highlands (Paracho-Paricutin region),
971 Presented at the Pre-meeting field guide for the 5th international Maar Conference, Querétaro,
972 México, pp. 1–37: 2014.

973 Sigala, I., Caballero, M., Correa-Metrio, A., Lozano-García, S., Vázquez, G., Pérez, L., Zawisza, E.: Basic
974 limnology of 30 continental waterbodies of the Transmexican Volcanic Belt across climatic and
975 environmental gradients, *Bol. Soc. Geológica Mex.*, 69, 313–370,
976 <https://doi.org/10.18268/BSGM2017v69n2a3>, 2017.

977 Silva-Aguilera, R.A., Vilaclara, G., Armienta, M.A., Escolero, Ó.: Hydrogeology and Hydrochemistry of
978 the Serdán-Oriental Basin and the Lake Alchichica, in: Alcocer, J. (Ed.), *Lake Alchichica Limnology*.
979 Springer International Publishing, Cham, pp. 63–74, https://doi.org/10.1007/978-3-030-79096-7_5,
980 2022.

981 Sperling, E.A., Peterson, K.J., Laflamme, M.: Rangeomorphs, Thectardis (Porifera?) and dissolved
982 organic carbon in the Ediacaran oceans: Rangeomorphs, Thectardis and DOC, *Geobiology*, 9, 24–33,
983 <https://doi.org/10.1111/j.1472-4669.2010.00259.x>, 2011.

984 Swanson-Hysell, N.L., Rose, C.V., Calmet, C.C., Halverson, G.P., Hurtgen, M.T., Maloof, A.C.:
985 Cryogenian Glaciation and the Onset of Carbon-Isotope Decoupling, *Science*, 328, 608–611,
986 <https://doi.org/10.1126/science.1184508>, 2010.

987 Thomas, P.J., Boller, A.J., Satagopan, S., Tabita, F.R., Cavanaugh, C.M., Scott, K.M.: Isotope
988 discrimination by form IC RubisCO from *Ralstonia eutropha* and *Rhodobacter sphaeroides*,
989 metabolically versatile members of ‘*Proteobacteria*’ from aquatic and soil habitats, *Environ.*
990 *Microbiol.*, 21, 72–80, <https://doi.org/10.1111/1462-2920.14423>, 2019.

991 Thornton, D.C.O.: Dissolved organic matter (DOM) release by phytoplankton in the contemporary
992 and future ocean, *Eur. J. Phycol.*, 49, 20–46, <https://doi.org/10.1080/09670262.2013.875596>, 2014.

- 993 Tziperman, E., Halevy, I., Johnston, D.T., Knoll, A.H., Schrag, D.P.: Biologically induced initiation of
994 Neoproterozoic snowball-Earth events, *Proc. Natl. Acad. Sci.*, 108, 15091–15096,
995 <https://doi.org/10.1073/pnas.1016361108>, 2011.
- 996 Vilaclara, G., Chávez, M., Lugo, A., González, H., Gaytán, M.: Comparative description of crater-lakes
997 basic chemistry in Puebla State, Mexico, *Internationale Vereinigung für theoretische und*
998 *angewandte Limnologie: Verhandlungen*, 25, 435–440,
999 <https://doi.org/10.1080/03680770.1992.11900158>, 1993.
- 1000 Wagner, S., Schubotz, F., Kaiser, K., Hallmann, C., Waska, H., Rossel, P.E., Hansman, R., Elvert, M.,
1001 Middelburg, J.J., Engel, A., Blattmann, T.M., Catalá, T.S., Lennartz, S.T., Gomez-Saez, G.V., Pantoja-
1002 Gutiérrez, S., Bao, R., Galy, V.: Soothsaying DOM: A Current Perspective on the Future of Oceanic
1003 Dissolved Organic Carbon, *Front. Mar. Sci.*, 7, 341, <https://doi.org/10.3389/fmars.2020.00341>, 2020.
- 1004 Werne, J.P., Hollander, D.J.: Balancing supply and demand: controls on carbon isotope fractionation
1005 in the Cariaco Basin (Venezuela) Younger Dryas to present, *Mar. Chem.*, 92, 275–293,
1006 <https://doi.org/10.1016/j.marchem.2004.06.031>, 2004.
- 1007 Wetz, M.S., Wheeler, P.A.: Release of dissolved organic matter by coastal diatoms, *Limnol.*
1008 *Oceanogr.*, 52, 798–807, <https://doi.org/10.4319/lo.2007.52.2.0798>, 2007.
- 1009 Williams, P.M., Gordon, L.I.: Carbon-13: carbon-12 ratios in dissolved and particulate organic matter
1010 in the sea, *Deep Sea Res. Oceanogr. Abstr.*, 17, 19–27, [https://doi.org/10.1016/0011-7471\(70\)90085-](https://doi.org/10.1016/0011-7471(70)90085-9)
1011 9, 1970.
- 1012 Xing, C., Liu, P., Wang, R., Li, C., Li, J., Shen, B.: Tracing the evolution of dissolved organic carbon
1013 (DOC) pool in the Ediacaran ocean by Germanium/silica (Ge/Si) ratios of diagenetic chert nodules
1014 from the Doushantuo Formation, South China, *Precambrian Res.*, 374, 106639,
1015 <https://doi.org/10.1016/j.precamres.2022.106639>, 2022.
- 1016 Zeebe, R.E., Wolf-Gladrow, D.A.: Carbon Dioxide, Dissolved (Ocean). In: Gornitz, V. (eds) *Encyclopedia*
1017 *of Paleoclimatology and Ancient Environments. Encyclopedia of Earth Sciences Series.* Springer,
1018 Dordrecht, https://doi.org/10.1007/978-1-4020-4411-3_30, 2009.
- 1019 Zeyen, N., Benzerara, K., Beyssac, O., Daval, D., Muller, E., Thomazo, C., Tavera, R., López-García, P.,
1020 Moreira, D., Duprat, E.: Integrative analysis of the mineralogical and chemical composition of modern
1021 microbialites from ten Mexican lakes: What do we learn about their formation? *Geochim.*
1022 *Cosmochim. Ac.*, 305, 148–184, <https://doi.org/10.1016/j.gca.2021.04.030>, 2021.